ORIGINAL RESEARCH

Rac1 Modulates Endothelial Function and Platelet Aggregation in Diabetes Mellitus

Gabriele Giacomo Schiattarella, MD, PhD;* Albino Carrizzo, PhD;* Federica Ilardi, MD; Antonio Damato, BSc; Mariateresa Ambrosio, BSc; Michele Madonna, DVM, PhD; Valentina Trimarco, PhD; Marina Marino, MSc; Elena De Angelis, MD; Silvio Settembrini, MD; Cinzia Perrino, MD, PhD; Bruno Trimarco, MD; Giovanni Esposito, MD, PhD; Carmine Vecchione, MD

***Background*—**Vascular complications and abnormal platelet function contribute to morbidity and mortality in diabetes mellitus. We hypothesized that the Rho-related GTPase protein, Rac1, can influence both endothelial and platelet function and might represent a potential novel therapeutic target in diabetes mellitus.

***Methods and Results*—**We used both in vitro and ex vivo approaches to test the effects of pharmacological inhibition of Rac1 during hyperglycemic condition. We evaluated the effect of NSC23766, a pharmacological inhibitor of Rac1, on vascular function in diabetic mice and platelet aggregation in diabetic subjects. We demonstrated that the administration of NSC23766 protects from hyperglycemia-induced endothelial dysfunction, restoring NO levels, and reduces oxidative stress generated by nicotinamide adenine dinucleotide phosphate oxidase. Mechanistically, we identified Rho-associated coiled-coil serine/threonine kinase-1 as a downstream target of Rac1. Moreover, we reported that during hyperglycemic conditions, human platelets showed hyperactivation of Rac1 and impaired NO release, which were both partially restored after NSC23766 treatment. Finally, we characterized the antiplatelet effect of NSC23766 during hyperglycemic conditions, demonstrating the additional role of Rac1 inhibition in reducing platelet aggregation in diabetic patients treated with common antiplatelet drugs.

***Conclusions*—**Our data suggest that the pharmacological inhibition of Rac1 could represent a novel therapeutic strategy to reduce endothelial dysfunction and platelet hyperaggregation in diabetes mellitus. **(*J Am Heart Assoc*. 2018;7:e007322. DOI: 10.1161/JAHA.117.007322.)**

Key Words: endothelial dysfunction • NO • oxidative stress • cardiovascular disease • vascular reactivity

Macrovascular and microvascular complications contribute to morbidity and mortality in diabetes mellitus.[1–3] Endothelial dysfunction and abnormal platelet function represent the main determinants of the vascular accidents in diabetic patients, contributing to high incidence of thrombotic events.[4] Chronic hyperglycemia observed in type 2 diabetes mellitus induces platelet activation and increases reactive oxygen species (ROS) production in endothelium, playing an important role in the development of vascular damage.[5,6]

The small GTPase Rac1 is essential for the correct assembly of nicotinamide adenine dinucleotide phosphate oxidase (Nox) subunits.[7] Several pathways converge in the activation of Rac1, and some evidence suggests a role in different cellular mechanisms, such as cell adhesion, chemotaxis, and vascular permeability.[7] In addition to its role in ROS

From the Department of Advanced Biomedical Sciences, Federico II University, Naples, Italy (G.G.S., F.I., E.D.A., C.P., B.T., G.E.); IRCCS Neuromed, Pozzilli (Isernia), Italy (A.C., A.D., M.A., M. Madonna, C.V.); Hypertension Research Center, Federico II University Hospital, Naples, Italy (V.T.); Presidio Ospedaliero Umberto I, Nocera Inferiore (Salerno), Italy (M. Marino); Servizio Diabetologia e Malattie Metaboliche, ASL Napoli 1 Centro, Naples, Italy (S.S.); and Department of Medicine and Surgery, University of Salerno, Baronissi (Salerno), Italy (C.V.).

Accompanying Data S1, Tables S1, S2, and Figures S1 through S7 are available at http://jaha.ahajournals.org/content/7/8/e007322/DC1/embed/inline-supplementary-material-1.pdf

Correspondence to: Carmine Vecchione, MD, Vascular Physiopathology Unit, IRCCS Neuromed, Pozzilli (IS) 86077, Italy.
Department of Medicine and Surgery, University of Salerno, Via S Allende, Baronissi (SA) 84081, Italy. E-mail: cvecchione@unisa.it
Giovanni Esposito, MD, PhD, Division of Cardiology, Department of Advanced Biomedical Sciences, Federico II University, Via S Pansini 5, Naples 80131, Italy. E-mail: espogiov@unina.it

Received August 4, 2017; accepted February 14, 2018.

Clinical Perspective

What Is New?

- The molecular mechanisms that govern endothelial dysfunction and enhanced platelet aggregation in diabetes mellitus are not completely elucidated.
- Herein, we show that Rac1 participates in diabetes mellitus–induced platelet alterations and endothelial dysfunction.

What Are the Clinical Implications?

- Rac1 inhibition reduces platelet hyperactivity and endothelial dysfunction in diabetes mellitus.
- Therefore, Rac-1 could represent a potential therapeutic target to ameliorate both pathophysiological alterations in diabetes mellitus.

generation in endothelium, Rac1 represents a key orchestrator of platelet actin cytoskeleton, modulating, in turn, platelet aggregation.[8] The role of Rac1 in hyperglycemia-induced platelet hyperaggregation is still poorly understood.

Antiplatelet drugs, such as aspirin, are prescribed to diabetic patients for prevention of ischemic cardiovascular diseases; however, many patients exhibit "aspirin resistance" with a high rate of cardiovascular events.[9–11] Furthermore, despite optimal antiplatelet therapy, many patients exhibit high residual platelet reactivity, which has been associated with higher risk of cardiovascular events as well.[12] Therefore, even a small variation in platelet activity might precipitate thrombotic events. This indicates the necessity of identifying new molecular targets to limit platelet aggregation in diabetes mellitus. In this regard, Rac1 could represent a good candidate able to modulate both endothelial function and platelet aggregation. Recently, a small molecule able to inhibit Rac1 activity, named NSC23766, has been developed.[13,14] NSC23766 has been shown to inhibit Rac1 activity by interfering with its binding domain involved in the determination of Rac1's specificity to a subset of guanine nucleotide exchange factors that catalyze the exchange of GDP to GTP to maintain Rac1 in its active, GTP-bound, form.[14,15] Recently, we have shown the beneficial effects of Rac1 inhibition through NSC23766 on endothelial dysfunction in human vessels.[16] However, the mechanisms by which NSC23766 exerts its protective role on endothelial function in hyperglycemia are still partially unknown.

Rho-associated coiled-coil serine/threonine kinase-1 (ROCK1) is the main downstream target of the small GTPase RhoA and has been involved in the regulation of multiple cellular functions involving cytoskeletal organization.[17] Given the important role of Rac1 in endothelial and platelet function, we hypothesized that ROCK1 might represent a potential downstream target of Rac1 activity.

To better understand the role of Rac1 in diabetes mellitus, we investigated the possible therapeutic role of NSC23766 on vascular and platelet alteration using both in vitro and ex vivo approaches in preclinical model of diabetes mellitus and human samples.

Methods

The data, analytic methods, and study materials will be made available to other researchers for purposes of reproducing the results or replicating the procedure on request to corresponding authors. All experiments involving animals were conformed to the *Guide for the Care and Use of Laboratory Animals* published by the US National Institutes of Health (publication 85-23, revised 2011) and were approved by the Istituto di Ricovero e Cura a Carattere Scientifico Istituto Neurologico Mediterraneo Neuromed review board. Human subjects were enrolled at the Cardiology Division of the University of Naples Federico II. The study protocol was conformed to the principles outlined in the Declaration of Helsinki and was approved by the institutional review board of the medical center, and each patient who accepted to participate provided written informed consent. All diabetic patients enrolled in our study fulfilled the criteria of the

Table. Baseline Characteristics of the Study Subjects

Characteristics	Control Subjects (n=11)	Diabetic Subjects (n=22)
Age, y	56.3±5.03	57.05±2.39
Women, %	36	30
Hypertension, %	40	35
Hyperlipidemia, %	22	25
BMI, kg/m^2	24.17±1.1	26.13±1.12
Smoking, %	46	45
HbA1c, %	5.5±0.31	8.3±1.32*
Drug therapy, n		
Statins	0	0
ACEIs	6	10
ARBs	6	10
CCBs	5	10
BBs	4	5
Anticoagulants	0	0
ASA	0	7
Other antiplatelet agents	0	0

Data are represented as mean±SD unless otherwise indicated. ACEI indicates angiotensin-converting enzyme inhibitor; ARB, angiotensin receptor blocker; ASA, acetylsalicylic acid; BB, β blocker; BMI, body mass index; CCB, calcium channel blocker; and HbA1c, glycated hemoglobin.
*P=0.00012 vs control subjects.

National Diabetes Data Group for diabetes mellitus.[18] Characteristics of patients (demographics, concomitant medication therapy, and glycemic status) are summarized in the Table and Table S1. An expanded description of materials and methods used in this study is available in Data S1.

Statistical Analysis

Data are presented as bar graphs, box-and-whisker plots, or points and connecting line. Plots show mean, and the error bars represent SEM. Different data sets were generated to test differences in the experiments involving animals/cells or humans. In the animal/cells study, differences were analyzed by Mann-Whitney nonparametric test to compare 2 independent groups or by Kruskal-Wallis test in experiments including ≥3 groups. For vascular reactivity studies, differences were analyzed using nonparametric Friedman test, followed by Dunn's multiple comparison test, for the analysis of the effects of the pharmacological treatments on vascular reactivity function. Human data were presented as mean and SD and analyzed by 2-tailed Student *t* test (Table). No randomization was applied to allocate patients in the different groups because diabetic patients were chosen on the basis of glycated hemoglobin percentage (baseline difference). Therefore, no adjustment in the analysis was made because of the baseline differences. No repeated measurements on the same experimental unit over time were used. All experiments can be considered on different experimental units. A minimum value of $P<0.05$ was considered statistically significant. All statistical analyses were conducted using GraphPad Prism software 7.0.

Results

Rac1 Inhibition Protects From Endothelial Dysfunction in a Mouse Model of Diabetes Mellitus

To evaluate the effects of NSC23766 on vascular function in diabetes mellitus, we used a previously described mouse model of streptozotocin-induced diabetes mellitus.[19] Mesenteric arteries were isolated from streptozotocin-treated mice and their control (vehicle-injected) littermates after IP injection of NSC23766 (5 mg/kg, as previously described),[20,21] at different time points (6, 12, 24, 36, 48, and 96 hours after injection) to perform vascular reactivity studies (Figure 1A through 1F). No effects on blood glucose levels and body weight were found after NSC23766 treatment in both control and streptozotocin-treated mice (Table S2).

As expected, diabetes mellitus caused impaired endothelial vasorelaxation, as demonstrated by reduced response to acetylcholine in mesenteric arteries of mice treated with streptozotocin (Figure 1). In contrast, smooth muscle relaxation induced by nitroglycerine was unaffected by diabetes mellitus (data not shown). Interestingly, in vivo administration of NSC23766 in streptozotocin-treated mice reduced endothelial dysfunction, ameliorating vasorelaxation starting after 6 hours from injection, with a sustained effect present up to 96 hours after administration (Figure 1A through 1F).

As expected, diabetic arteries also exhibited increased ROS production and Nox activity (Figure 2A). We also observed that, in streptozotocin-treated mice, both mRNA and protein levels of ROCK1 were increased (Figure 2B and 2C), coupled with significant downregulation of phosphoinositide 3-kinase/protein kinase B signaling pathway (Figure 2C). Interestingly, NSC23766 treatment abolished Rac1 activation in diabetic vessels, which, in turn, reduced RhoA and ROCK1 levels, restoring the phosphoinositide 3-kinase/protein kinase B signaling pathway and endothelial NO synthase (eNOS) phosphorylation (Figure 2B). These data support the role of Rac1 as an upstream modulator of ROCK1 involved in eNOS dysfunction and ROS production in diabetes mellitus.

NSC23766 Prevents High Glucose–Induced Endothelial Dysfunction by Restoring eNOS Phosphorylation and Reducing Oxidative Stress

To evaluate the in vitro effects of NSC23766 on glucose-induced endothelial dysfunction, mesenteric arteries from wild-type C57BL/6 mice were treated with 2 different glucose concentrations, mimicking normoglycemia (5 mmol/L) or hyperglycemia (25 mmol/L). Vessels exposed to 25 mmol/L of glucose for 30 minutes showed a significant reduction of acetylcholine-evoked vasorelaxation compared with vessels treated with 5 mmol/L of glucose (Figure 3A), whereas no differences between the 2 different doses of glucose were found in nitroglycerine-induced vasorelaxation (Figure S1). These data confirm the detrimental effects of high glucose levels on vascular function. Interestingly, pretreatment with Rac1 inhibitor, NSC23766 (30 μmol/L), was able to protect from endothelial dysfunction induced by high glucose (Figure 3A), restoring eNOS phosphorylation and reducing ROS production and Nox activity (Figure 3B and 3C).

ROCK1 Is Involved in Rac1-Dependent Effects on Vascular Function

It has been reported that Rac1 negatively modulates eNOS function.[22] This mechanism appears to be likely mediated by the reduction of ROCK1, a negative regulator of eNOS. In fact, ROCK1 inhibits eNOS gene expression and inhibits phosphoinositide 3-kinase/protein kinase B signaling, which phosphorylates and activates eNOS.[23,24] Accordingly, vessels treated with high glucose concentration in presence of

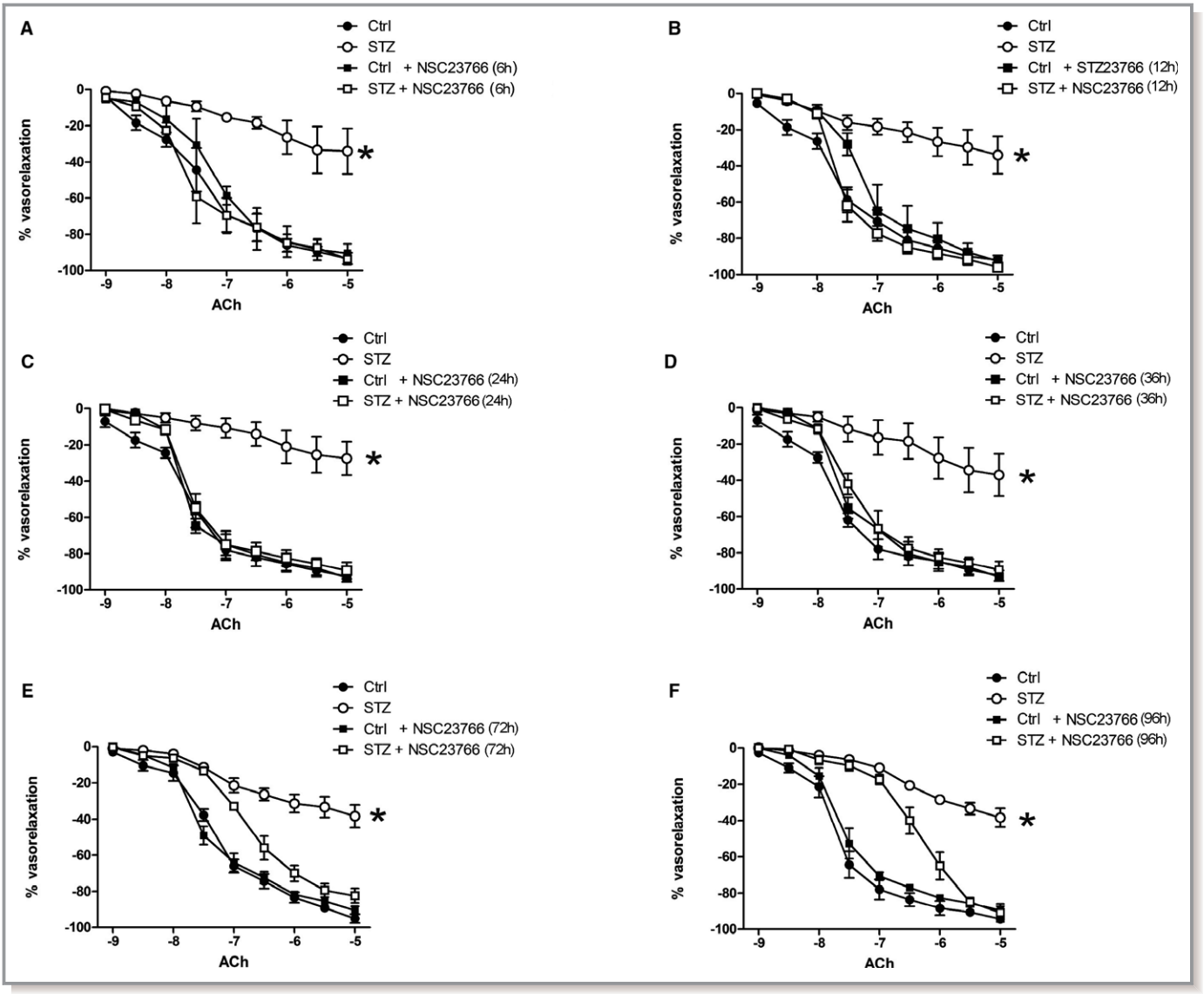

Figure 1. NSC23766 restores relaxation in diabetic vessels. Acetylcholine (ACh) vasorelaxation in preconstricted mesenteric arteries from vehicle-treated mice (control [Ctrl]; full circles), streptozotocin-treated mice (STZ; empty circles), from Ctrl mice treated with Rac1 inhibitor (Ctrl+NSC23766; full squares), and from STZ-treated mice plus Rac1 inhibitor (STZ+NSC23766; empty squares) at different time points from single injection of NSC23766: 6 hours (A), 12 hours (B), 24 hours (C), 36 hours (D), 48 hours (E), and 96 hours (F). n=4 for each group. **P*<0.05 vs all.

LY27632, an inhibitor of ROCK1 activity, showed increased eNOS phosphorylation and enhanced vasorelaxation compared with vessels treated with high glucose alone (Figure 3B and 3D). Notably, in LY27632-treated vessels, Rac1 was still activated, positioning it as an upstream modulator of ROCK1 (Figure 3B). Although the administration of Rac1 inhibitor in presence of LY27632 did not further enhance eNOS phosphorylation compared with LY27632 alone (Figure 3B), at functional level it was able to potentiate endothelial vasorelaxation, suggesting that additional mechanism(s) are recruited by Rac1 inhibitor to modulate endothelial function (Figure 3D). Interestingly, in the same model of hyperglycemia-induced vascular damage, inhibition of Rac1 but not inhibition of ROCK1 was able to protect the arteries from high glucose–induced ROS generation, as shown by a significant reduction in Nox levels after treatment with NSC23766 (Figure 3C).

To better evaluate the contribution of ROS in the differential response on vascular function observed with Rac1 and ROCK1 inhibitors, the antioxidant agent tiron (10^{-3} mol/L), a superoxide scavenger, was used in addition to ROCK1 inhibitor. Treatment with tiron+LY27632 restored endothelial vasorelaxation at similar level observed in presence of Rac1 inhibitor (Figure 3E). On the contrary, the addition of tiron to NSC23766 did not influence the vascular response evoked by Rac1 inhibition in presence of high glucose levels, whereas

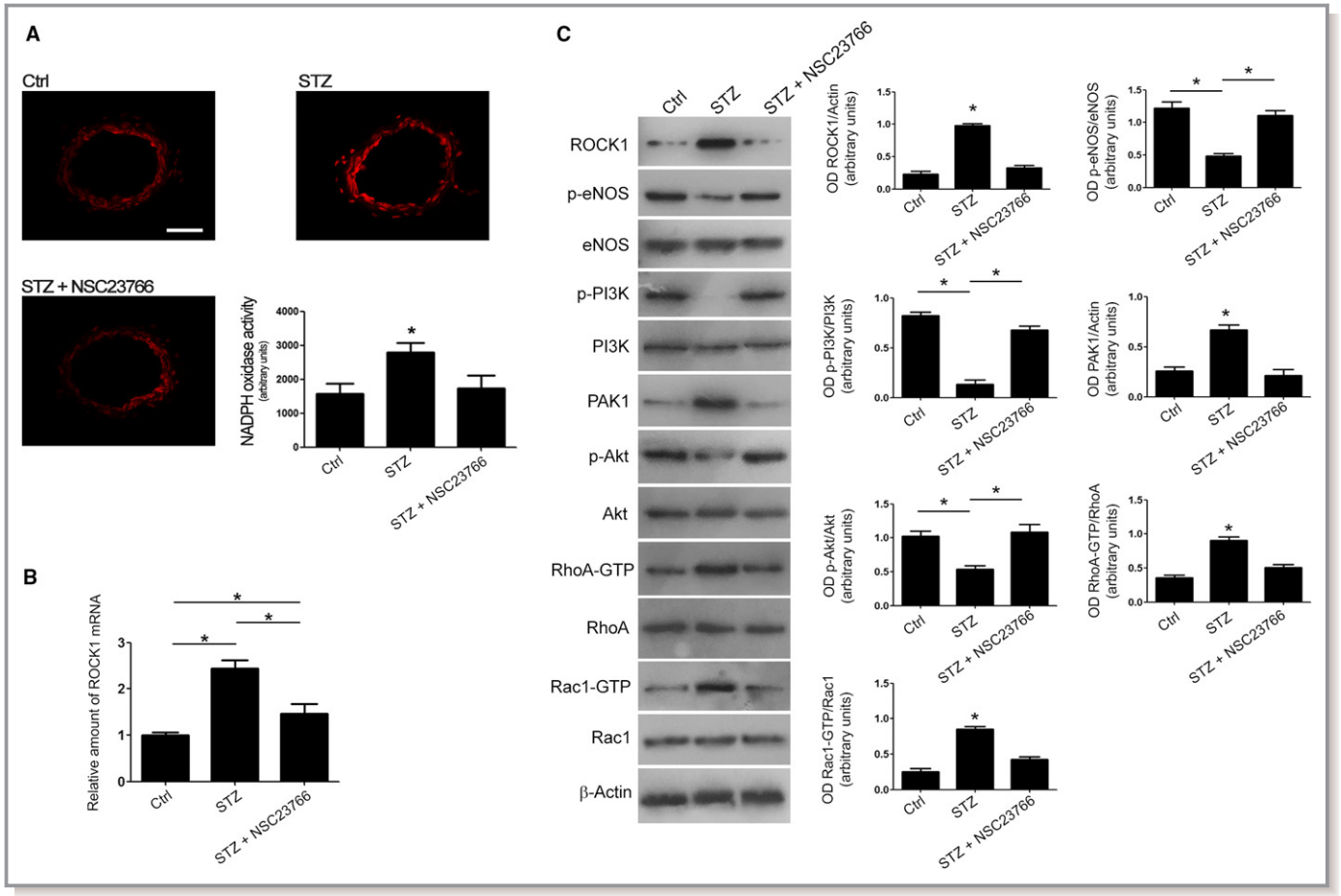

Figure 2. NSC23766 restores endothelial NO synthase (eNOS) function and reduces reactive oxygen species in diabetic vessels. A, Representative micrographs of Dihydroethidium staining to evaluate oxidative stress in mesenteric arteries from mice treated with vehicle (control [Ctrl]), with streptozotocin (STZ), or with streptozotocin plus NSC23766 (STZ+NSC23766; 48 hours). Representative images (n=3). Columns represent the effect of NSC23766 on nicotinamide adenine dinucleotide phosphate (NADPH)–induced lucigenin chemiluminescence in STZ mice mesenteric arteries. Data are expressed as increase of chemiluminescence per minute in arbitrary units. n=4 for each group. **P*<0.05 vs all. B, The mRNA levels of Rho-associated coiled-coil serine/threonine kinase-1 (ROCK1) were determined by quantitative reverse transcription–polymerase chain reaction in vessels from Ctrl, STZ, and STZ+NSC23766, 48 hours. n=3 for each group. **P*<0.05. C, Representative immunoblots (left) and densitometric analysis (right) of 4 independent experiments evaluating protein levels of ROCK-1, phospo (p)-eNOS, eNOS, p-phosphoinositide 3-kinase (PI3K), PI3K, p-protein kinase B (Akt; T473), Akt, p21 activated kinase, RhoA-GPT, RhoA, Rac1-GTP, Rac1, and β-actin in mesenteric arteries from Ctrl, STZ, and STZ+NSC23766 mice, 48 hours. n=3 for each group. **P*<0.05.

treatment with tiron alone only partly ameliorated vascular relaxation, accordingly with its scavenger effects (Figure 3E).

Given the striking reduction of ROS production and Nox activity observed after NSC23766 treatment, we aimed to determine the individual contribution of different Nox isoforms in glucose-induced ROS generation. Interestingly, the use of Nox4 inhibitor, GTK137831, significantly decreased ROS production and Nox activity in glucose-treated vessels (Figure 3C), whereas no effects were observed after treatment with Nox1 inhibitor, ML-171 (Figure 3C). We also observed that Nox4 inhibition by GTK137831 partially restored acetylcholine-induced vasorelaxation in mesenteric arteries treated with high glucose dose (Figure 3F). Interestingly, treatment of dysfunctional vessels with Nox1 inhibitor ML-171 did not improve vascular reactivity (Figure 3F). These data demonstrate a specific involvement of Nox4 isoform in glucose-induced ROS production and suggest that the observed vascular antioxidant effects of NSC23766 could be mediated, at least in part, by the inhibition of Nox4 isoform of Nox.

The beneficial effects of Rac1/ROCK1 inhibition on glucose-induced endothelial dysfunction and ROS production observed in the whole vessels were also observed in human endothelial cells (Figure S2). Collectively, these data demonstrate that ROCK1 inhibition ameliorates, in part, hyperglycemia-induced endothelial dysfunction without affecting ROS production, whereas the improvement of endothelial function observed with Rac1 inhibitor is also attributable to its inhibitor effect on Nox, primarily on Nox4 isoform, reducing ROS production.

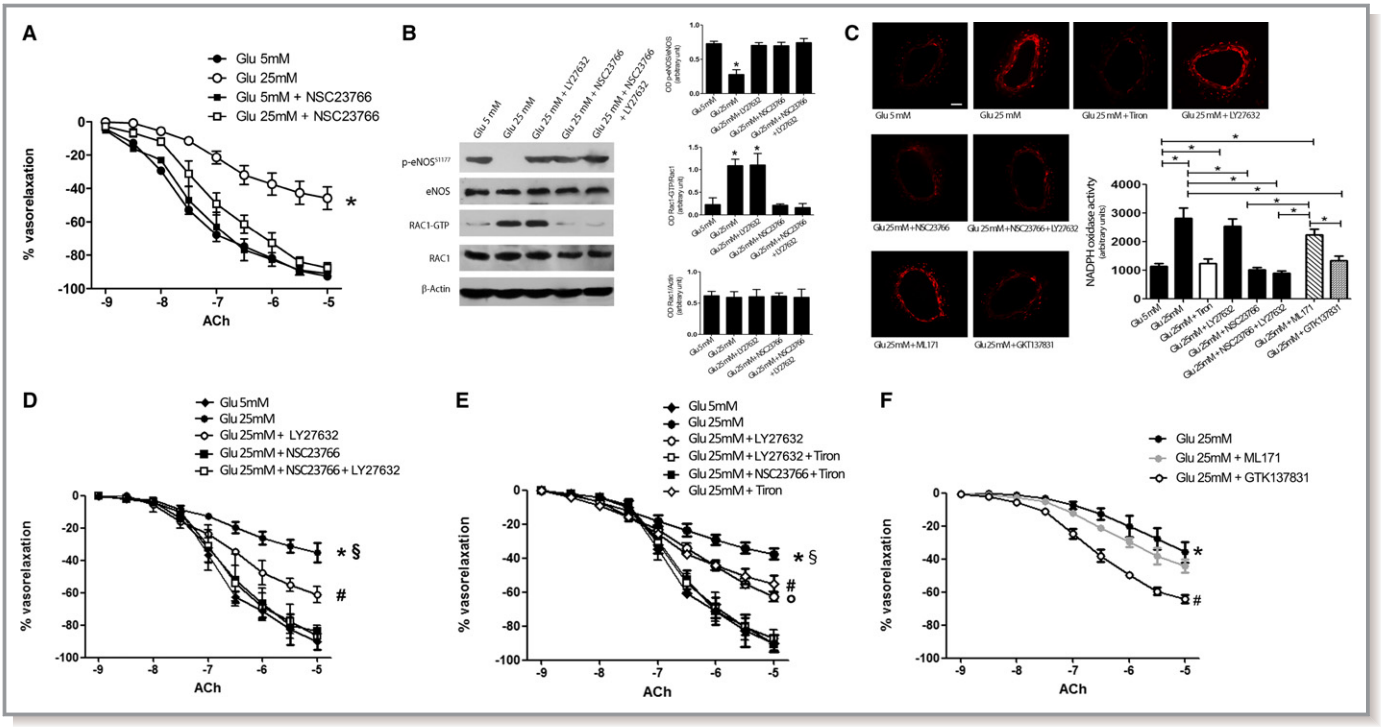

Figure 3. Interplay between RAC1 and Rho-associated coiled-coil serine/threonine kinase-1 in vessels and platelets. A, Acetylcholine (ACh) vasorelaxation in preconstricted mesenteric arteries treated with low glucose (Glu; 5 mmol/L; full circles), high glucose (Glu 25 mmol/L; empty circles), low glucose plus Rac1 inhibitor (Glu 5 mmol/L+NSC23766; full squares), and high glucose plus Rac1 inhibitor (Glu 25 mmol/L+NSC23766; empty squares). n=4 for each group. **P*<0.05 vs all. B, Representative immunoblots (left) and densitometric analysis (right) of 4 independent experiments evaluating protein levels of p-endothelial NO synthase (eNOS), eNOS, Rac1-GTP, total Rac1, and β-actin in mesenteric arteries treated with Glu 5 mmol/L, Glu 25 mmol/L, Glu 25 mmol/L plus LY27632 (Glu 25 mmol/L+LY27632), Glu 25 mmol/L+NSC23766, or Glu 25 mmol/L+NSC23766+LY27632. **P*<0.05 vs all; **P*<0.05 vs Glu 5 mmol/L, Glu 25 mmol/L+NSC23766, and Glu 25 mmol/L+NSC23766+LY27632. C, Representative images of Dihydroethidium staining to evaluate oxidative stress in mesenteric arteries treated with different stimuli/inhibitors. Columns represent the effect of NSC23766, LY27632, GKT137831, and ML-171 on nicotinamide adenine dinucleotide phosphate (NADPH)–induced lucigenin chemiluminescence in mice mesenteric arteries. Data are expressed as increase of chemiluminescence per minute in arbitrary units. n=4 for each group. **P*<0.05. D, ACh vasorelaxation in preconstricted mesenteric arteries from control treated with Glu 5 mmol/L, Glu 25 mmol/L, Glu 25 mmol/L+LY27632, Glu 25 mmol/L+NSC23766, and Glu 25 mmol/L+NSC23766+LY27632. n=4 for each group. **P*<0.05 vs Glu+LY27632; $^{\#}$*P*<0.05 vs Glu 5 mmol/L, Glu 25 mmol/L+NSC23766, and Glu 25 mmol/L+NSC23766+LY27632; §*P*<0.05 vs Glu 5 mmol/L, Glu 25 mmol/L+NSC23766, and Glu 25 mmol/L+NSC23766+LY27632. E, ACh vasorelaxation in preconstricted mesenteric arteries from mesenteric arteries treated with Glu 5 mmol/L, Glu 25 mmol/L, Glu 25 mmol/L+LY27632, Glu 25 mmol/L+LY27632+tiron, Glu 25 mmol/L+NSC23766+tiron, and Glu 25 mmol/L+tiron. n=3 for each group. **P*<0.05 vs Glu 25 mmol/L+LY27632; $^{\#}$*P*<0.05 vs Glu 5 mmol/L, Glu 25 mmol/L+LY27632+tiron, and Glu 25 mmol/L+NSC23766+tiron; §*P*<0.05 vs Glu 5 mmol/L, Glu 25 mmol/L+LY27632+tiron, and Glu 25 mmol/L+NSC23766+tiron; $^{\circ}$*P*<0.05 vs Glu 5 mmol/L, Glu 25 mmol/L+LY27632+tiron, and Glu 25 mmol/L+NSC23766+tiron. F, ACh vasorelaxation in preconstricted mesenteric arteries from vessels treated with Glu 25 mmol/L, Glu 25 mmol/L plus ML-171 (Glu 25 mmol/L+ML-171), or Glu 25 mmol/L plus GTK137831 (Glu 25 mmol/L+GTK137831. n=5 for each group. **P*<0.05 vs Glu25 mmol/L+GTK137831; $^{\#}$*P*<0.05 vs Glu 25 mmol/L+ML-171.

Rac1 Inhibition Restores NO Production in High Glucose–Treated Human Platelets

Treatment of human platelets with high glucose concentration (25 mmol/L) induced a strong activation of Rac1 and a significant reduction of eNOS phosphorylation (Figure 4A). Interestingly, administration of LY27632 restored eNOS phosphorylation without affecting Rac1 activation (Figure 4A), posing Rac1 as an upstream modulator of ROCK1 signaling also in platelets. In addition, NSC23766 was also able to restore eNOS phosphorylation, in presence of high glucose, at similar levels compared with LY27632, whereas coadministration of both Rac1 and ROCK1 inhibitors did not further modify eNOS phosphorylation status (Figure 4A). These data suggested that the effect of NSC23766 on eNOS phosphorylation is mediated by ROCK1.

Reduced platelet NO production represents a crucial alteration in diabetes mellitus. As expected, we observed a dramatic impairment of NO release in the supernatants of platelets exposed to high glucose concentration compared with platelets exposed to low glucose, measured by Sievers NO analyzer (NOA280i) (Figure 4B). To confirm the specificity of

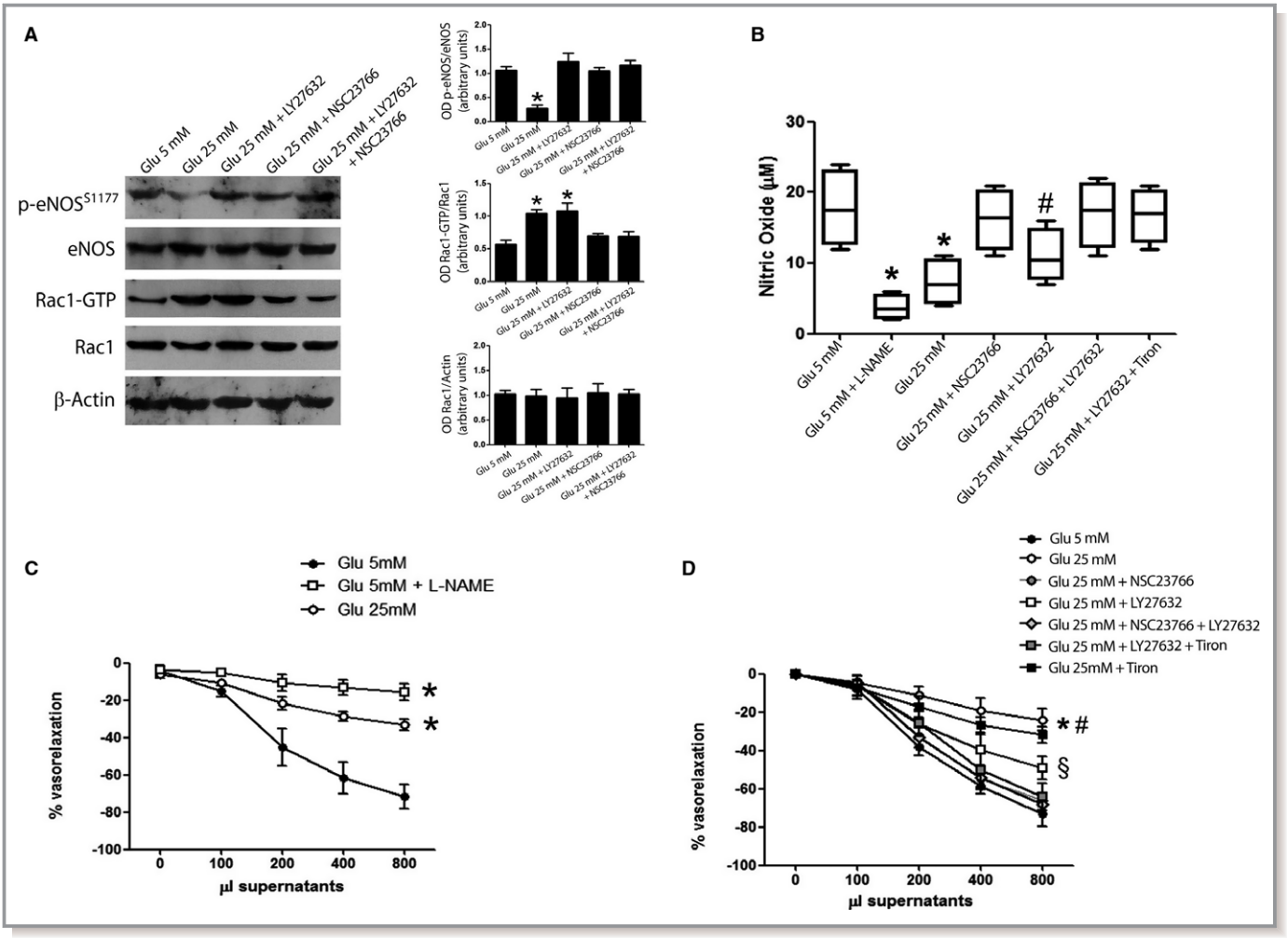

Figure 4. Rac1 inhibition restores NO release from platelets. A, Representative immunoblots (left) and densitometric analysis (right) of 4 independent experiments evaluating protein levels of p-endothelial NO synthase (eNOS), eNOS, Rac1-GTP, total Rac1, and β-actin in platelets. **P*<0.05 vs all. B, Quantitative measurement of NO levels in platelet supernatants treated with glucose 5 mmol/L (Glu 5 mmol/L), Glu 5 mmol/L+Nω-nitro-L-arginine methyl ester hydrochloride (L-NAME), glucose 25 mmol/L (Glu 25 mmol/L), Glu 25 mmol/L plus NSC23766 (Glu 25 mmol/L+NSC23766), Glu 25 mmol/L plus LY27632 (Glu 25 mmol/L+LY27632), Glu 25 mmol/L plus NSC23766 plus LY27632 (Glu 25 mmol/L+NSC23766+LY27632), and Glu 25 mmol/L plus LY27632 plus tiron (Glu 25 mmol/L+LY27632+tiron). Box plots representing the mean and the minimum and maximum values of NO amounts. n=4 for each group. **P*<0.05 vs all; $^{\#}$*P*<0.05 vs Glu 25 mmol/L+NSC23766, Glu 25 mmol/L+NSC23766+LY27632, Glu 5 mmol/L, and Glu 25 mmol/L. C, Dose-response curves of phenylephrine precontracted aorta rings to supernatants derived from human platelets treated with Glu 5 mmol/L, Glu 5 mmol/L+L-NAME, and Glu 25 mmol/L. n=4 for each group. **P*<0.05 vs Glu 5 mmol/L. D, Dose-response curves of phenylephrine precontracted aorta rings to supernatants derived from human platelets treated with Glu 5 mmol/L, Glu 25 mmol/L, Glu 25 mmol/L+NSC23766, Glu 25 mmol/L+LY27632, Glu 25 mmol/L+NSC23766+LY27632, Glu 25 mmol/L+LY27632+tiron, or Glu 25 mmol/L+tiron. n=4 for each group. **P*<0.05 vs all; §*P*<0.05 vs Glu 25 mmol/L+LY27632; §*P*<0.05 vs Glu 25 mmol/L+NSC23766; $^{\#}$*P*<0.05 vs all.

NO production, we also measured NO levels in supernatant of platelets treated with NOS inhibitor Nω-nitro-L-arginine methyl ester hydrochloride. As shown in Figure 4B, Nω-nitro-L-arginine methyl ester hydrochloride treatment completely abolished NO production in platelet supernatant. Interestingly, treatment with Rac1 inhibitor NSC23766 restored platelet NO production, whereas treatment of high glucose–stimulated platelets with ROCK1 inhibitor was able to restore only, in part, the impaired NO production (Figure 4B). Similar to what was observed in vessels, addition of tiron to high-glucose platelets treated with LY27632 further enhanced NO production to the levels observed with Rac1 inhibitor NSC23766 (Figure 4B).

Human platelet supernatant evoked a rapid dose-dependent relaxation of mouse aortic rings; this effect was NO dependent because it was abolished by eNOS inhibition with Nω-nitro-L-arginine methyl ester hydrochloride (Figure 4C). As expected, the effect on vasorelaxation induced by platelet supernatant was markedly reduced by high glucose level (25 mmol/L) compared with vessels treated with supernatant of platelets with low dose of glucose (5 mmol/L) (Figure 4C),

confirming the effects of high glucose to induce an impairment in the NO-dependent vasorelaxant mechanisms.

To evaluate the role of Rac1/ROCK1 axis in platelet-induced NO-dependent vasorelaxation, supernatants from NSC23766 or ROCK1 inhibitor LY27632-treated platelets were used on mouse aortic ring preparations. Interestingly, treatment of platelets with NSC23766 restored the ability of platelet supernatant to induce a dose-dependent relaxation of mouse aortic rings in presence of high glucose levels (Figure 4D), whereas the supernatant of LY27632-treated platelets was able to ameliorate only, in part, vasorelaxation (Figure 4D). Interestingly, the addition of tiron caused an enhancement of vasorelaxant effect observed with supernatant of LY27632-treated platelets, reaching a similar level on what was observed in presence of NSC23766 alone or NSC23766 plus LY27632 (Figure 4D). The administration of tiron alone exerted only a mild, not significant, improvement of vasorelaxation.

Taken together, these results indicated that the effect of Rac1 inhibitor on NO metabolism in presence of high glucose levels depends on the modulation of both eNOS phosphorylation and oxidative stress.

NSC23766 Reduces Platelet Aggregation Induced by High Glucose Levels

Because impairment of NO production is closely associated with an increase of platelet reactivity, we investigated the effect of Rac1 inhibitor on human platelet aggregation. As expected, platelet aggregation induced by type I collagen was enhanced after treatment with increasing concentrations of glucose (Figure 5A). Subsequently, we aimed to identify the effective concentration of NSC23766 able to modulate platelet aggregation. We performed a dose-response curve with NSC23766 in human platelets exposed to 5 and 25 mmol/L of glucose. In platelets exposed to 5 mmol/L (mimicking "normoglycemic" condition), the effective dose to reach a significant inhibition of platelet aggregation was 30 μmol/L, whereas further increase in NSC23766 dose (starting from 50 μmol/L) practically abolished any collagen-induced aggregation (Figure 5B). Interestingly, when the same dose-response curve was done exposing platelets to 25 mmol/L of glucose (mimicking "hyperglycemic" condition), an increased sensitivity to Rac1 inhibition was observed. Specifically, under this condition, the inhibitory effect of NSC23766 on platelet aggregation appeared already at the dose of 15 μmol/L, decreasing further at 30 μmol/L (Figure 5B). Similar results were obtained when platelets were stimulated with different agonists, such as arachidonic acid (0.5 mmol/L), ADP (50 mmol/L), or thrombin receptor-activating peptide (25 μmol/L) (data not shown). These results suggest that glucose per se can prime platelets, making them more susceptible to the effects of NSC23766, and that Rac1 hyperactivity played a pivotal role in the modulation of high glucose–induced platelet aggregation.

Moreover, to demonstrate that Rac1 effects on glucose-dependent platelet aggregation were not dependent by changes in platelet osmolarity, we evaluated platelet aggregation after increasing dose of osmotic-control mannitol with and without NSC23766. The administration of mannitol did not change platelet reactivity, confirming the specific role of glucose to induce platelet hyperaggregation (Figure S3). Accordingly, platelet Rac1 levels did not show any change after mannitol treatment (Figure S3).

Finally, we investigated the potential role of ROCK1 in modulation of platelet aggregation during hyperglycemic conditions. Differently from what was observed in vessels, ROCK1 inhibition by LY27632 in platelets did not affect platelet aggregation in presence of both high glucose or low glucose concentrations (data not shown), confirming the marginal role of ROCK1 in modulation of platelet aggregation, as observed before.[25]

Platelets From Diabetic Patients Show Increased Levels of Activated Rac1

To translate our results into a clinical setting, we evaluated active Rac1 levels in platelets isolated from diabetic patients and control subjects without diabetes mellitus (Table). Platelets from diabetic patients showed higher levels of activated Rac1 compared with control samples (Figure 6A and 6B).

It is well known that in diabetes mellitus, platelets are hyperreactive, with intensified adhesion, activation, and aggregation.[26] Thus, we evaluated the level of activated Rac1 in platelets from diabetic patients accordingly with their reported percentage of glycated hemoglobin. Interestingly, our pull-down assay showed a higher level of active Rac1 in platelets from patients with elevated percentage of glycated hemoglobin (10%) compared with those with lower glycated hemoglobin (7%), indicating a correlation between diabetes mellitus status and Rac1 activation (Figure 6A and 6B).

Moreover, to evaluate the effect of diabetes mellitus on platelets, we evaluated platelet aggregation in diabetic patients. As expected, under basal condition, the aggregation induced by collagen was enhanced in platelets from diabetic patients compared with control subjects (Figure 6C, left panel). Next, we evaluated the efficacy of NSC23766 to inhibit collagen-induced platelet activation in diabetic patients. Interestingly, to obtain a significant reduction in diabetic platelet aggregation, a higher dose of NSC23766 was necessary compared with control platelets (60 in comparison to 30 μmol/L already effective in platelets from control subjects) (Figure 6C, middle panel).

Although platelets exposed to increasing concentration of glucose exhibit an increased sensitivity to Rac1 inhibition

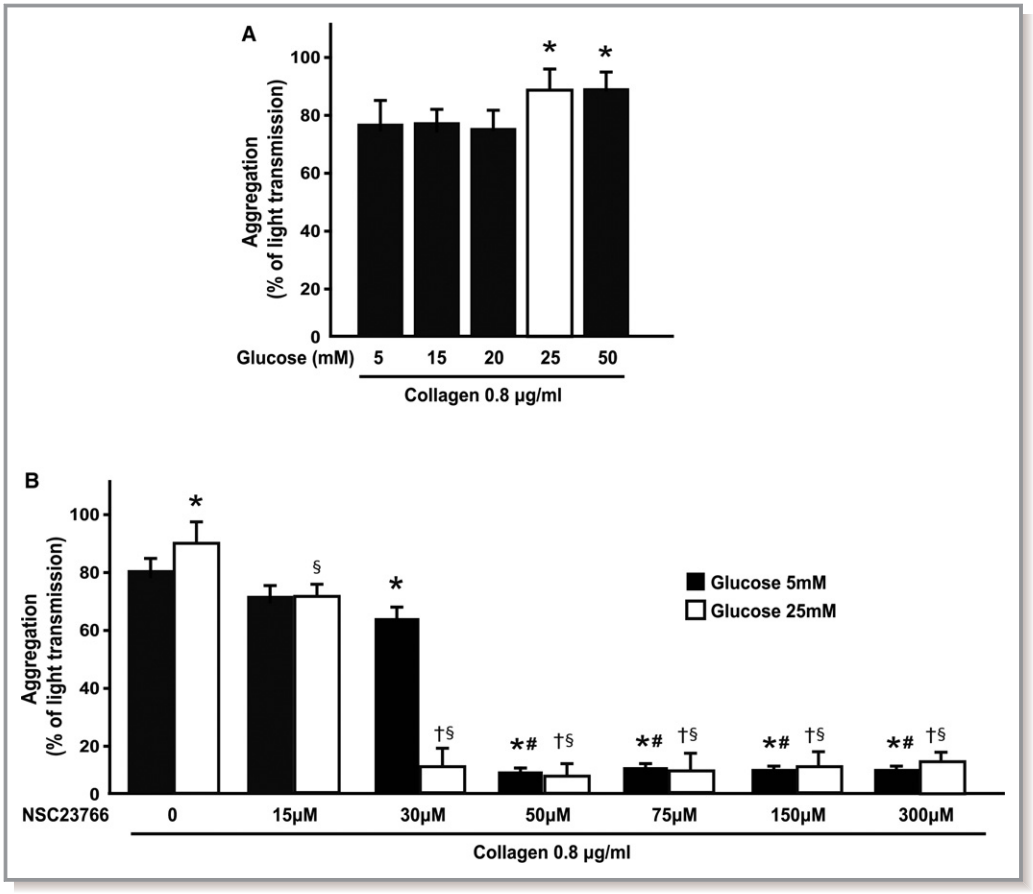

Figure 5. NSC23766 inhibits glucose-induced platelet hyperaggregation. A, Quantification of platelet aggregation presented as percentage of light transmission of platelets from control (CTRL) subjects treated with increasing concentrations of glucose (Glu). n=6 independent experiments from individual subjects. **P*<0.05 vs glucose 5 mmol/L. B, Quantification of platelet aggregation presented as percentage of light transmission of platelets from CTRL subjects treated with increasing concentrations of NSC23766 at 5 and 25 mmol/L Glu. n=4 independent experiments from individual subjects. **P*<0.05 vs Glu 5 mmol/L without NSC23766; #*P*<0.05 vs Glu 5 mmol/L with NSC23766 30 µmol/L; §*P*<0.05 vs Glu 25 mmol/L without NSC23766; †*P*<0.05 vs Glu 25 mmol/L with NSC23766 15 µmol/L and Glu 5 mmol/L with NSC23766 30 µmol/L.

(Figure 5B), higher doses of Rac1 inhibitor were necessary to reach the same levels of inhibition of aggregation in platelets isolated from diabetic patients (Figure 6C, middle panel). To rule out the potential off-target effects of NSC23766 observed when used at high concentrations,[27] we used another structurally different Rac1 inhibitor, called EHT1864. As shown in Figure S4, also with EHT1864, a higher dose of inhibitor was necessary to significantly reduce platelet aggregation in diabetic conditions compared with control subjects.

NSC23766 Exerts Additive Effect on Platelet Aggregation From Diabetic Patients Treated With Acetylsalicylic Acid

On the basis of the evidence that several diabetic patients showed a resistance to common antiplatelet drugs, such as acetylsalicylic acid (ASA), we decided to investigate the efficacy of NSC23766 treatment in isolated platelets from ASA-treated diabetic patients. In particular, we tested increasing concentrations of NSC23766 on platelets from diabetic patients treated with ASA, 100 mg/d. Interestingly, in this experimental condition, NSC23766 treatment was able to further reduce the platelet aggregation in diabetic patients already treated with ASA (Figure 6C, right panel).

Discussion

We found that pharmacological inhibition of Rac1 by NSC23766 attenuated endothelial dysfunction in experimental model of diabetes mellitus and reduced platelet hyperaggregation in diabetic patients. These novel results suggest a potential protective role of Rac1 inhibition on vascular injury and platelet hyperaggregation in diabetes mellitus.

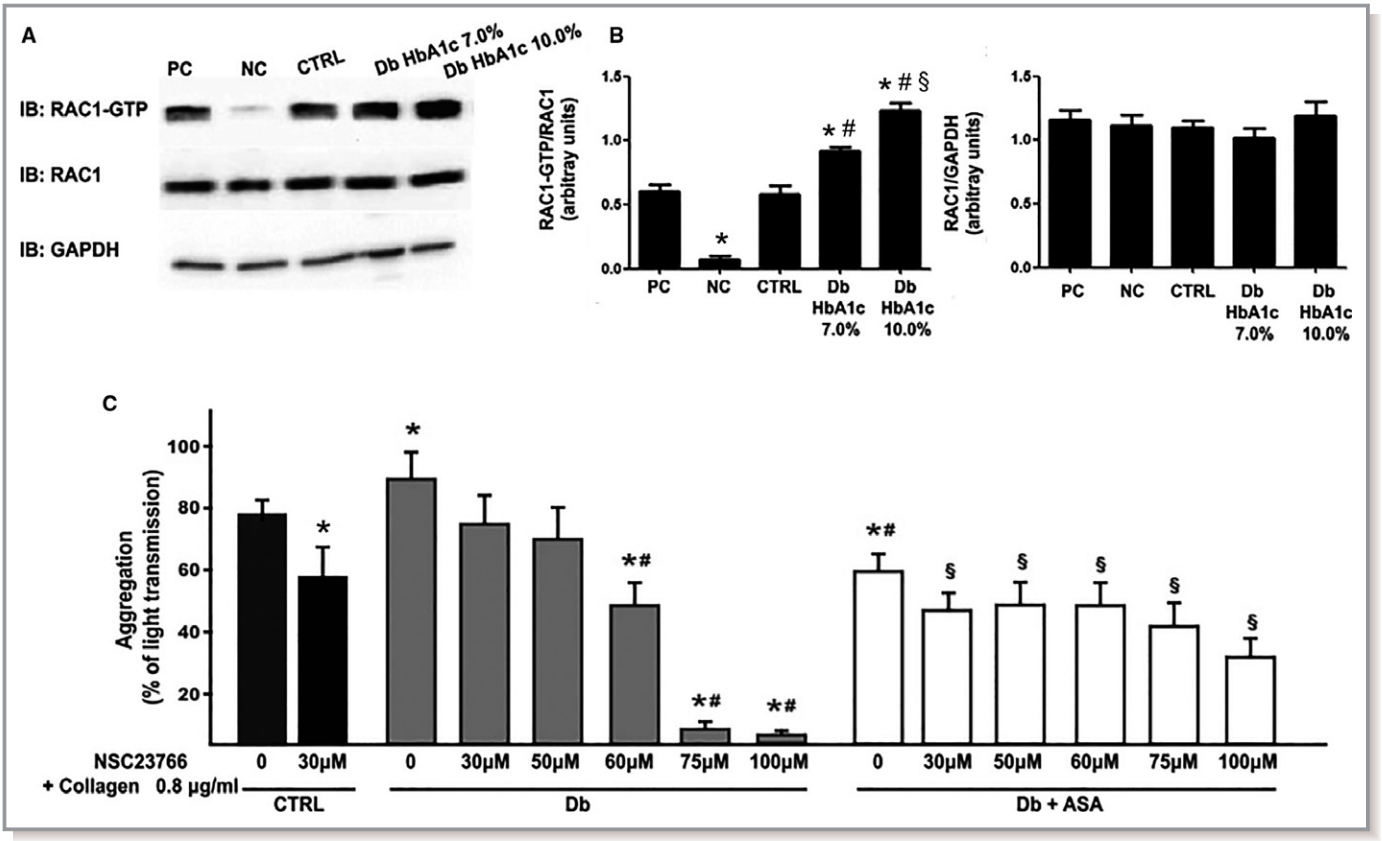

Figure 6. NSC23766 ameliorates platelet hyperaggregation in diabetes mellitus. A, Representative immunoblots of Rac1-GTP and Rac1 levels in platelets from control (CTRL) subjects or diabetic (Db) patients with different percentage of glycated hemoglobin (HbA1c). GAPDH protein levels were used for normalizing samples. B, Densitometric analysis of Rac1-GTP (left) and Rac1 (right) protein levels in platelet samples from CTRL and Db patients. n=4 independent experiments from individual subjects. **P*<0.05 vs all; #*P*<0.05 vs CTRL; §*P*<0.05 vs Db HbA1c 7.0%. C, Quantification of platelet aggregation presented as percentage of light transmission of CTRL platelets (left), Db platelets (middle), and Db platelets+acetylsalicylic acid (ASA) treated with NSC23766. n=4 independent experiments from individual subjects. **P*<0.05 vs CTRL 0 (without NSC23766); #*P*<0.05 vs Db 0 (without NSC23766); §*P*<0.05 vs CTRL, Db 0, and Db+ASA 0 (without NSC23766). IB indicates immunoblot; NC, negative control; and PC, positive control.

Rac1 is a regulatory component of Nox, which represents 1 of the major sources of ROS in the vascular wall. ROS generation is crucially involved in diabetes mellitus and diabetic complications.[28] Although many sources of ROS contribute to increased oxidative stress in diabetes mellitus (direct effect of hyperglycemia, mitochondria, and xanthine oxidase), several Nox isoforms have been found specifically upregulated in vascular wall in the presence of high glucose.[29,30] We have previously shown that Rac1 represents a crucial modulator of ROS-induced vascular dysfunction in preclinical model of diabetes mellitus.[19] Its inhibition by an adenoviral vector carrying Rac1 dominant negative mutant protects from endothelial dysfunction in experimental diabetes mellitus.[19] In the past decade, NSC23766 was identified as a small-molecule inhibitor of Rac–guanine nucleotide exchange factor–mediated activation of Rac1.[14,15] Until now, its main field of application has been cancer biology, in which Rac1 has been reported as a novel important therapeutic target in several type of malignancies.[31–35] Given the growing importance of Rac1 in the cardiovascular system, recently NSC23766 has been tested in different cardiovascular disorders.[22]

Herein, we have shown the protective effects of Rac1 inhibitor, NSC23766, on endothelial function after high glucose–induced vascular damage. Mechanistically, we demonstrated that amelioration of endothelial function via restoration of eNOS phosphorylation by Rac1 inhibition requires ROCK1 as a crucial component of Rac1 signaling in both isolated cells and vessels. Although previous studies have suggested a reduction in eNOS expression after Rac1 inhibition,[36] the modulation of Rac1 activity by NSC23766 in our study was not related to changes in its expression in both mouse vessels and human endothelial cells. Moreover, we were recently able to demonstrate that Rac1 inhibition by NSC23766 exerts a beneficial effect also in human vessels, ameliorating endothelial dysfunction.[16] These results pointed out the important role of Rac1 as a therapeutic target to improve vascular homeostasis.

Levay et al[27] have demonstrated an effect of NSC23766 as nonselective competitive antagonist of muscarinic acetylcholine receptors in neonatal rat cardiomyocytes. In our experimental model on resistance vessels, we were able to show that NSC23766 per se did not interfere with acetylcholine vasorelaxation (Figure S5). Consistently with other studies, we have demonstrated that the activation of Rac1 (Rac1-GTP) negatively modulates eNOS phosphorylation through ROCK-1 pathway.[37,38] In addition to its effect on eNOS phosphorylation, inhibition of Rac1 also blunted Nox ROS production. Hence, these data demonstrated that the amelioration of endothelial relaxation obtained by Rac1 inhibition in presence of high glucose levels depends on 2 mechanisms: the increased eNOS phosphorylation and the reduction of oxidative stress.

These data prompted us to explore the effects of Rac1 inhibitor in a mouse model of diabetes mellitus. NSC23766 treatment reduced the enhanced Rac1 activation observed in preclinical diabetes mellitus and restored acetylcholine-evoked vasorelaxation. Interestingly, amelioration of endothelial function observed after Rac1 inhibition in vessels from diabetic mice was present up to 96 hours after NSC23766 systemic administration and, accordingly, we observed a sustained inhibition of Rac1 activity in mice vessels at the same time point (Figure S6). Reduction of ROS production in diabetic vessels treated with NSC23766 can be attributed to reduction in Nox activity. Although, given the complexity of ROS production in diabetes mellitus, previously discussed, it is likely that Nox might not be the only target of Rac1 inhibition. Using pharmacological inhibition of the different Nox isoform, we were able to identify Nox4 as a critical component of NSC23766-mediated ROS suppression in vascular wall. These data will serve as a platform to pursue more in-depth mechanistic insights in Rac1/Nox4 interaction.

In addition to vascular damage, diabetes mellitus is also characterized by platelet dysfunction. Previous studies reported that high levels of glucose were able to increase platelet aggregation in vitro and were associated with ROS production.[39] Rac1 is involved in platelet actin cytoskeleton reorganization during platelet activation. A crucial feature of platelets is represented by their ability to produce NO. Our data demonstrate that high glucose levels activate Rac1 in platelets, and this effect is associated with an impaired NO release. Notably, similar to what was observed in vessels and endothelial cells, the administration of NSC23766 in platelets protects from the deleterious effect of high glucose on NO metabolism, enhancing eNOS phosphorylation, through ROCK-1 inhibition, and blunting oxidative stress. It is well known that a reduction in NO release is coupled with alteration in platelet activation. In this regard, 1 of the most striking changes that occur during platelet activation is the translocation of CD62 (P-selectin) protein to the outer platelet membrane. Therefore, the expression of CD62 on the membrane of platelets is considered to be a valuable indicator for platelet activation in different diseases, including diabetes mellitus.[40,41] To evaluate the effects of NSC23766 on platelet activation in diabetes mellitus, we performed the immunoblot analysis of CD62 expression in cytosol and membrane subcellular fraction of platelets isolated from diabetic (streptozotocin-treated) and control mice in presence and absence of NSC23766. As shown in Figure S7, membrane expression of CD62 in diabetic platelets was significantly increased. More important, in vivo administration of NSC23766 in diabetic mice abolished CD62 membrane translocation in platelets, demonstrating a significant reduction of platelet activation on Rac1 inhibition. These data suggest that the effects of NSC23766 on platelet function in diabetes mellitus are potentially beyond the expected cytoskeleton reorganization and might contribute to the beneficial effects observed in vitro and in vivo, corroborating our previous results.

Interestingly, herein we have shown that Rac1 is responsive to high glucose levels, enhancing platelet aggregation, acknowledging Rac1 as an important regulator of platelet function during hyperglycemic conditions. We demonstrated that a condition mimicking hyperglycemia in vitro increases platelet Rac1 activation. On the basis of this result, we hypothesized that increased active Rac1 platelet levels under hyperglycemic conditions could contribute to the increased platelet activity observed in diabetes mellitus. Using a specific inhibitor of Rac1 activity, NSC23766, we demonstrated that glucose-induced platelet hyperaggregation was reduced. The increased efficacy of NSC23766 to inhibit platelet aggregation in hyperglycemic state could be explained by increased Rac1 GTP levels under this condition. The effect of glucose on platelet aggregation starts to appear for concentration of glucose of 25 mmol/L and seems to be sustained even with higher concentration (50 mmol/L), suggesting the presence of a threshold for glucose-induced hyperaggregation in human platelets. Under normal glucose condition, the dose of 30 μmol/L, NSC23766 was sufficient to reduce Rac1 activity, modulating, in turn, platelet function. Although the dose used in our study was significantly lower compared with the one used elsewhere,[42] we cannot completely exclude that the potential off-target effects of NSC23766 might affect our results. Because the effect of NSC23766 on platelet aggregation, under high glucose condition, is already present for lower NSC23766 doses (15 μmol/L), this raised the question of how to separate the effect of hyperglycemia and the effect of NSC23766 on platelet aggregation. In our experiments, we chose relatively high levels of glucose (25 and 50 mmol/L) to mimic hyperglycemic conditions. Indeed, these levels of hyperglycemia are clinically relevant, because blood glucose commonly increases at ≈30 mmol/L in diabetic ketoacidosis and can reach 60 mmol/L during diabetic hyperosmolar

coma.[43] Therefore, during hyperglycemic condition, even a small increase in platelet aggregation can significantly worsen the clinical conditions. In our experiments, we recorded an increase of ≈10% in platelet aggregation on hyperglycemic stimuli using light transmission aggregometry. This increase is consistent with previous literature using the same technique,[39] although it can be smoothened by the fact that the baseline percentage of platelet aggregation in our subjects is higher compared with previous reports. We speculated that this effect can be attributable to the fact that the control population is not represented by completely "healthy" subjects because, despite being free from cardiovascular disease and diabetes mellitus, they present some cardiovascular risk factors, such as hypertension and smoking, that can contribute to the increased platelet reactivity. Collectively, data from other groups and we suggest that hyperglycemic condition produces a 10% to 20% increase in platelet aggregation after stimulation with proaggregating stimuli (ie, collagen) that can reflect, at least in part, the prothrombotic state observed in diabetic patients.

Given the known off-target effect of NSC23766,[42] it is possible to speculate that glucose can prime platelets, making them more susceptible to the effects of NSC23766. Accordingly, in our model, Rac1 GTP is specifically induced by high glucose in platelets, without osmotic effects, as demonstrated by the absence of Rac1 activation with mannitol; therefore, the mild effects of NSC23766 on platelet aggregation observed in normoglycemic state might be caused by the low levels of Rac1 GTP in platelets. Accordingly, platelets from diabetic patients showed a positive correlation between activated Rac1 and levels of glycated hemoglobin. To provide further support that Rac1 is a critical target in diabetic platelets, we used another Rac1 inhibitor, called EHT1864. Differently from NSC23766, which prevents the conversion of Rac1-GDP to Rac1-GTP by competitively blocking the binding loop of Rac1-specific guanine nucleotide exchange factors, EHT1864 is a specific allosteric inhibitor of the Rac family, resulting in dissociation of nucleotides.[44] Using 2 different Rac1 inhibitors, we further corroborate the notion that Rac1 plays a major role in platelet proaggregating status in diabetes mellitus, underlying the peculiar platelet characteristics of diabetic subjects.

It is important to underline that in condition of Rac1 hyperactivation (such as platelets from diabetic patients), a higher dose of Rac1 inhibitor was necessary to reduce platelet aggregation compared with platelets from subjects without diabetes mellitus, pointing out that diabetes mellitus affects platelet function in many ways, which are to be exclusively recapitulated by increasing the concentrations of glucose in vitro. We also found NSC23766 treatment further reduced platelet aggregation in those subjects taking ASA, identifying Rac1 inhibition as a potential future pharmacological strategy to limit platelet hyperaggregation in diabetes mellitus. Unlike diabetic patients without ASA in whom we were able to recognize a dose-response curve of Rac1 inhibitory effects on platelet aggregation, the additive effects of NSC23766 on ASA-treated diabetic platelets were not dose dependent. These effects could be attributed to the lower responsiveness of platelets already treated with ASA. In fact, inhibition of platelet aggregation by other mechanisms (such as cyclooxygenase-dependent mechanisms) could blunt the incremental inhibitory effect of Rac1 inhibition.

Study Limitations

The beneficial effects of Rac1 inhibition on hyperglycemia-induced vascular and platelet dysfunction observed ex vivo need to be confirmed in ad hoc preclinical models of thrombus formation and using tissue-specific genetic approaches to distinguish between platelet- and endothelial cell–driven effects. Nevertheless, the current findings suggest that Rac1 inhibition may be accomplished directly in vivo because of the favorable safety profile of NSC23766, as observed in our mouse model of streptozotocin-induced diabetes mellitus. Finally, the effects of LY27632 as ROCK1 inhibitor can be also attributed, in part, to the inhibition of ROCK2, although recent studies have demonstrated that ROCK1 and ROCK2 have distinct nonredundant functions and have different targets in different cell types.[45,46]

Conclusions

The results of our study address an important challenge in biological features of diabetes mellitus (namely, platelet hyperreactivity and endothelial dysfunction). We provide further evidence about the involvement of Rac1 in both vascular injury and platelet hyperaggregation induced by diabetes mellitus. Our findings could support the use of Rac1 inhibition by NSC23766 in combination with ASA for antiplatelet therapy in diabetes mellitus. Although proposing Rac1 inhibitor as an immediate therapeutic approach in diabetic patients is far beyond the scope of our work, we believe that the identification of targets/drugs able to modulate >1 function in this disease could represent the right way to move forward. In particular, the combination of beneficial effects of Rac1 inhibition on both vascular and platelet function in diabetes mellitus might represent a potential effective strategy (in the future) to increase the therapeutic compliance of these patients.

Sources of Funding

This study was supported in part by Programma Operativo Nazionale–Ricerca e Competitività 2007–2013 "Cardiotech-

tecnologie avanzate per l'innovazione e l'ottimizzazione dei processi, diagnostici terapeutici e di training dedicati alla gestione clinica, interventistica e riabilitativa dei paziente affetti da sindromi coronariche acute" (PON01_02833; Esposito).

Disclosures

None.

References

1. Beckman JA, Creager MA, Libby P. Diabetes and atherosclerosis: epidemiology, pathophysiology, and management. *JAMA*. 2002;287:2570–2581.
2. Morel O, Kessler L, Ohlmann P, Bareiss P. Diabetes and the platelet: toward new therapeutic paradigms for diabetic atherothrombosis. *Atherosclerosis*. 2010;212:367–376.
3. Ferreiro JL, Angiolillo DJ. Diabetes and antiplatelet therapy in acute coronary syndrome. *Circulation*. 2011;123:798–813.
4. Carr ME. Diabetes mellitus: a hypercoagulable state. *J Diabetes Complications*. 2001;15:44–54.
5. Cosentino F, Eto M, De Paolis P, van der Loo B, Bachschmid M, Ullrich V, Kouroedov A, Delli Gatti C, Joch H, Volpe M, Luscher TF. High glucose causes upregulation of cyclooxygenase-2 and alters prostanoid profile in human endothelial cells: role of protein kinase C and reactive oxygen species. *Circulation*. 2003;107:1017–1023.
6. Inoguchi T, Li P, Umeda F, Yu HY, Kakimoto M, Imamura M, Aoki T, Etoh T, Hashimoto T, Naruse M, Sano H, Utsumi H, Nawata H. High glucose level and free fatty acid stimulate reactive oxygen species production through protein kinase C—dependent activation of NAD(P)H oxidase in cultured vascular cells. *Diabetes*. 2000;49:1939–1945.
7. Carrizzo A, Forte M, Lembo M, Formisano L, Puca AA, Vecchione C. Rac-1 as a new therapeutic target in cerebro- and cardio-vascular diseases. *Curr Drug Targets*. 2014;15:1231–1246.
8. Akbar H, Kim J, Funk K, Cancelas JA, Shang X, Chen L, Johnson JF, Williams DA, Zheng Y. Genetic and pharmacologic evidence that Rac1 GTPase is involved in regulation of platelet secretion and aggregation. *J Thromb Haemost*. 2007;5:1747–1755.
9. Colwell JA. Aspirin for primary prevention of cardiovascular events in diabetes. *Diabetes Care*. 2003;26:3349–3350.
10. Colwell JA; American Diabetes Association. Aspirin therapy in diabetes. *Diabetes Care*. 2003;26(suppl 1):S87–S88.
11. Hankey GJ, Eikelboom JW. Aspirin resistance. *Lancet*. 2006;367:606–617.
12. Feldman L, Tubach F, Juliard JM, Himbert D, Ducrocq G, Sorbets E, Triantafyllou K, Kerner A, Abergel H, Huisse MG, Roussel R, Esposito-Farese M, Steg PG, Ajzenberg N. Impact of diabetes mellitus and metabolic syndrome on acute and chronic on-clopidogrel platelet reactivity in patients with stable coronary artery disease undergoing drug-eluting stent placement. *Am Heart J*. 2014;168:940–947.e5.
13. Akbar H, Cancelas J, Williams DA, Zheng J, Zheng Y. Rational design and applications of a Rac GTPase-specific small molecule inhibitor. *Methods Enzymol*. 2006;406:554–565.
14. Gao Y, Dickerson JB, Guo F, Zheng J, Zheng Y. Rational design and characterization of a Rac GTPase-specific small molecule inhibitor. *Proc Natl Acad Sci U S A*. 2004;101:7618–7623.
15. Gao Y, Xing J, Streuli M, Leto TL, Zheng Y. Trp(56) of rac1 specifies interaction with a subset of guanine nucleotide exchange factors. *J Biol Chem*. 2001;276:47530–47541.
16. Carrizzo A, Vecchione C, Damato A, di Nonno F, Ambrosio M, Pompeo F, Cappello E, Capocci L, Peruzzi M, Valenti V, Biondi-Zoccai G, Marullo AG, Palmerio S, Carnevale R, Spinelli CC, Puca AA, Rubattu S, Volpe M, Sadoshima J, Frati G, Sciarretta S. Rac1 pharmacological inhibition rescues human endothelial dysfunction. *J Am Heart Assoc*. 2017;6:e004746. DOI: 10.1161/JAHA.116.004746.
17. Riento K, Ridley AJ. Rocks: multifunctional kinases in cell behaviour. *Nat Rev Mol Cell Biol*. 2003;4:446–456.
18. National Diabetes Data Group. Classification and diagnosis of diabetes mellitus and other categories of glucose intolerance. *Diabetes*. 1979;28:1039–1057.
19. Vecchione C, Aretini A, Marino G, Bettarini U, Poulet R, Maffei A, Sbroggio M, Pastore L, Gentile MT, Notte A, Iorio L, Hirsch E, Tarone G, Lembo G. Selective Rac-1 inhibition protects from diabetes-induced vascular injury. *Circ Res*. 2006;98:218–225.
20. Hwaiz R, Hasan Z, Rahman M, Zhang S, Palani K, Syk I, Jeppsson B, Thorlacius H. Rac1 signaling regulates sepsis-induced pathologic inflammation in the lung via attenuation of Mac-1 expression and CXC chemokine formation. *J Surg Res*. 2013;183:798–807.
21. Zhang S, Rahman M, Song L, Herwald H, Thorlacius H. Targeting Rac1 signaling inhibits streptococcal M1 protein-induced CXC chemokine formation, neutrophil infiltration and lung injury. *PLoS One*. 2013;8:e71080.
22. Kisialiou A, Grella R, Carrizzo A, Pelone G, Bartolo M, Zucchella C, Rozza F, Grillea G, Colonnese C, Formisano L, Lembo M, Puca AA, Vecchione C. Risk factors and acute ischemic stroke subtypes. *J Neurol Sci*. 2014;339:41–46.
23. Ming XF, Viswambharan H, Barandier C, Ruffieux J, Kaibuchi K, Rusconi S, Yang Z. Rho GTPase/Rho kinase negatively regulates endothelial nitric oxide synthase phosphorylation through the inhibition of protein kinase B/Akt in human endothelial cells. *Mol Cell Biol*. 2002;22:8467–8477.
24. Eto M, Barandier C, Rathgeb L, Kozai T, Joch H, Yang Z, Luscher TF. Thrombin suppresses endothelial nitric oxide synthase and upregulates endothelin-converting enzyme-1 expression by distinct pathways: role of Rho/ROCK and mitogen-activated protein kinase. *Circ Res*. 2001;89:583–590.
25. Dasgupta SK, Le A, Haudek SB, Entman ML, Rumbaut RE, Thiagarajan P. Rho associated coiled-coil kinase-1 regulates collagen-induced phosphatidylserine exposure in platelets. *PLoS One*. 2013;8:e84649.
26. Brownlee M. Biochemistry and molecular cell biology of diabetic complications. *Nature*. 2001;414:813–820.
27. Levay M, Krobert KA, Wittig K, Voigt N, Bermudez M, Wolber G, Dobrev D, Levy FO, Wieland T. NSC23766, a widely used inhibitor of Rac1 activation, additionally acts as a competitive antagonist at muscarinic acetylcholine receptors. *J Pharmacol Exp Ther*. 2013;347:69–79.
28. Pitocco D, Tesauro M, Alessandro R, Ghirlanda G, Cardillo C. Oxidative stress in diabetes: implications for vascular and other complications. *Int J Mol Sci*. 2013;14:21525–21550.
29. Inoguchi T, Nawata H. NAD(P)H oxidase activation: a potential target mechanism for diabetic vascular complications, progressive beta-cell dysfunction and metabolic syndrome. *Curr Drug Targets*. 2005;6:495–501.
30. Sedeek M, Callera G, Montezano A, Gutsol A, Heitz F, Szyndralewiez C, Page P, Kennedy CR, Burns KD, Touyz RM, Hebert RL. Critical role of Nox4-based NADPH oxidase in glucose-induced oxidative stress in the kidney: implications in type 2 diabetic nephropathy. *Am J Physiol Renal Physiol*. 2010;299:F1348–F1358.
31. Guerriero L, Chong K, Franco R, Rosati A, De Caro F, Capunzo M, Turco MC, Hoon DS. BAG3 protein expression in melanoma metastatic lymph nodes correlates with patients' survival. *Cell Death Dis*. 2014;5:e1173.
32. Chen QY, Xu LQ, Jiao DM, Yao QH, Wang YY, Hu HZ, Wu YQ, Song J, Yan J, Wu LJ. Silencing of Rac1 modifies lung cancer cell migration, invasion and actin cytoskeleton rearrangements and enhances chemosensitivity to antitumor drugs. *Int J Mol Med*. 2011;28:769–776.
33. Heid I, Lubeseder-Martellato C, Sipos B, Mazur PK, Lesina M, Schmid RM, Siveke JT. Early requirement of Rac1 in a mouse model of pancreatic cancer. *Gastroenterology*. 2011;141:719–730, 730.e1–7.
34. Dokmanovic M, Hirsch DS, Shen Y, Wu WJ. Rac1 contributes to trastuzumab resistance of breast cancer cells: Rac1 as a potential therapeutic target for the treatment of trastuzumab-resistant breast cancer. *Mol Cancer Ther*. 2009;8:1557–1569.
35. Zuo Y, Shields SK, Chakraborty C. Enhanced intrinsic migration of aggressive breast cancer cells by inhibition of Rac1 GTPase. *Biochem Biophys Res Commun*. 2006;351:361–367.
36. Sawada N, Salomone S, Kim HH, Kwiatkowski DJ, Liao JK. Regulation of endothelial nitric oxide synthase and postnatal angiogenesis by Rac1. *Circ Res*. 2008;103:360–368.
37. Rikitake Y, Liao JK. Rho GTPases, statins, and nitric oxide. *Circ Res*. 2005;97:1232–1235.
38. Noma K, Oyama N, Liao JK. Physiological role of ROCKs in the cardiovascular system. *Am J Physiol Cell Physiol*. 2006;290:C661–C668.
39. Tang WH, Stitham J, Gleim S, Di Febbo C, Porreca E, Fava C, Tacconelli S, Capone M, Evangelista V, Levantesi G, Wen L, Martin K, Minuz P, Rade J, Patrignani P, Hwa J. Glucose and collagen regulate human platelet activity through aldose reductase induction of thromboxane. *J Clin Invest*. 2011;121:4462–4476.
40. Graff J, Klinkhardt U, Schini-Kerth VB, Harder S, Franz N, Bassus S, Kirchmaier CM. Close relationship between the platelet activation marker CD62 and the

granular release of platelet-derived growth factor. *J Pharmacol Exp Ther*. 2002;300:952–957.

41. Leytin V, Mody M, Semple JW, Garvey B, Freedman J. Quantification of platelet activation status by analyzing P-selectin expression. *Biochem Biophys Res Commun*. 2000;273:565–570.
42. Dutting S, Heidenreich J, Cherpokova D, Amin E, Zhang SC, Ahmadian MR, Brakebusch C, Nieswandt B. Critical off-target effects of the widely used Rac1 inhibitors NSC23766 and EHT1864 in mouse platelets. *J Thromb Haemost*. 2015;13:827–838.
43. Kasper DL, Harrison TR. *Harrison's Principles of Internal Medicine*. 16th ed. New York: McGraw-Hill, Medical Publishing. Division; 2005.
44. Onesto C, Shutes A, Picard V, Schweighoffer F, Der CJ. Characterization of EHT 1864, a novel small molecule inhibitor of Rac family small GTPases. *Methods Enzymol*. 2008;439:111–129.
45. Shi J, Wei L. Rho kinase in the regulation of cell death and survival. *Arch Immunol Ther Exp (Warsz)*. 2007;55:61–75.
46. Hahmann C, Schroeter T. Rho-kinase inhibitors as therapeutics: from pan inhibition to isoform selectivity. *Cell Mol Life Sci*. 2010;67:171–177.

SUPPLEMENTAL MATERIAL

Supplemental Methods

Experimental animals

All experiments involving animals were conform to the guidelines for the Care and Use of Laboratory Animals published from Directive 2010/63/EU of the European Parliament and were approved by IRCCS INM Neuromed review board (ref. number 1070/2015 PR). Diabetes was induced by four intraperitoneal injection (i.p. – once a day) of streptozotocin (STZ, 40 mg/kg body weight and dissolved in 0.1 M citrate buffer, pH 4.5) in male wild-type C57BL/6 mice (weighing approximately 25g). Control mice received citrate buffer alone (vehicle). Three days after the last injection of STZ, blood glucose levels were measured using glucose test strips (Roche) and mice with blood glucose at least 3-fold higher than the pre-injection level were used as diabetic mice. Mice were housed in groups (4–6 mice per cage) in a specific pathogen-free controlled environment (inverted 12 h light cycle; lights off at 10:00 hours). All mice had free access to standard mice chow and water. The experiments were conducted after 4 weeks following the induction of diabetes. Animals that have not developed diabetes were excluded from the study. NSC23766 (Tocris Biosceince) was injected in mice i.p. at the dose of 5 mg/kg. This dose was chosen on the basis of a pilot study conducted in our laboratory and taking into account previously published data [1, 2]. Mice were euthanized by intraperitoneal injection of 150 mg/kg Ketamine, 20mg/Kg xylazine.

Human studies

In our clinical study two population of patients were enrolled: 1) subjects without type-2 diabetes (CTRL, n=11) and 2) subjects with type-2 diabetes (Db, n=22). All the experiments used to evaluate platelets aggregation were carried in these two populations using the CTRL group as a reference. Table 1 describes the baseline characteristics of both populations. Subjects were enrolled at the Cardiology division of the University of Naples Federico II. The study protocol was approved by the institutional review board of the medical center, and each patient who accept to participate provided written informed consent. All Db patients enrolled in our study fulfilled the criteria of National

Diabetes Data Group for diabetes [3]. Diabetes developed in most of the patients after 40 years of age. None of the subject enrolled in both the two populations (CTRL and Db) had a history of coronary heart disease, recent myocardial infarction, unstable angina pectoris, heart failure, thyroid, renal, or hepatic disease. Pharmacological therapy is presented in Tale 1. A subgroup of 7 Db patients of the 22 enrolled were treated with ASA 100 mg daily and platelets aggregation were performed on blood samples 14 days after treatment as described before.

Vascular reactivity studies

Vessels were placed in a wire myograph system filled with glucose-free Krebs solution. First, an analysis of vascular reactivity curves was performed. In particular, vasoconstriction was assessed with 80 mmol/L of KCl or with increasing doses of phenylephrine (from 10^{-9} M to 10^{-6} M) or U46619 (10^{-11} M to 10^{-6} M), in control conditions. Vascular responses were then tested before and after glucose treatment (5-25 mM). Endothelium-dependent and -independent relaxation was assessed by measuring the dilatory responses of mesenteric arteries to cumulative concentrations of acetylcholine (from 10^{-9} M to 10^{-5} M) or nitroglycerine (from 10^{-9} M to 10^{-5} M), respectively, in vessels pre-contracted with phenylephrine at a dose necessary to obtain a similar level of pre-contraction in each ring (80% of initial KCl-evoked contraction). Caution was taken to avoid endothelial damage; functional integrity was reflected by the response to acetylcholine (from 10^{-9} M to 10^{-6} M). Some studies were performed treating the vessels with NSC23766 (30 µmol/L) or with ML171 (0,5 µmol/L) or with GTK137831 (1 µmol/L) . Vascular relaxation is reported as percentage, considering basal tension before phenylephrine stimulus as -100% of vascular relaxation and phenylephrine-induced tension as 0% of vascular relaxation.

Cell culture

Commercially available human umbilical veins endothelial cells (HUVECs) were purchased from Lonza (Walkersville, MD, USA) and grown in EBM-2 basal medium. Cells were used within the five passage and at 70% confluence for the following sets of experiments. The cells were treated with 5 mM or 25 mM of glucose for 24 hours, subsequently were treated with NSC23766 30μM or LY27632 30μM for 30 minutes. For the western blot experiments, cells were treated with acetylcholine 100 μmol/L for the last 15 minutes.

Measurement of NADPH oxidase activity

HUVECs was depleted of serum and prepared for the assay. Vessels were isolated and prepared for the assay. Cells were treated with 0 mM, 5 mM and 25 mM of glucose and then with NSC23766, 30μM for 30 minutes. At the end of treatment (1 hours) cells were resuspended at 2×10^6 cells/ml confluency in aerated balanced salt solution. 1×10^6 cells/ml were used for the assay. Cells from various treatments were added to a scintillation vial containing lucigenin (5 μmol/L) in the aerated balanced salt solution. After a 5-minute dark adaptation, photon emission was measured for 10 min using the Beckman LS6500 Multipurpose Scintillation counter measuring single photon emission. First, photon emission was measured using a buffer blank and dark-adapted lucigenin. NADPH (100 μmol/L) was added after measurement of background lucigenin chemiluminescence and measurements were performed for other 10 minutes.

Platelet experiments

Platelet isolation

Venous blood was drawn from peripheral antecubital vein in fasting without refrain from smoking volunteers at University Federico II of Naples, who were free from medication known to interfere with platelet function (CTRL group). Other blood samples were drawn from diabetic patients free or in treatment acetylsalicylic acid (ASA) 100 mg per day (Db and Db+ASA group). Platelet-rich plasma

(PRP) was prepared from blood (about 15 ml) that was drawn by venipuncture into 3 ml of 3.8% trisodium citrate (w/v). PRP was obtained by centrifugation of blood at 150 g at 25°C for 15 minutes and was used as source of platelets. Platelet-poor plasma (PPP) was prepared from the residual blood by centrifugation of the rest of the blood at 1400 g at 25°C for 10 minutes.

Study of vascular reactivity evoked by platelets supernatant

Platelet pellets were produced by centrifugation of PRP at 900 g for 7 minutes, and re-suspended in Tyrode's solution (132 mmol/L NaCl, 4 mmol/L KCl, 1.6 mmol/L $CaCl_2$, 0.98 $MgCl_2$, 23.8 mmol/L $NaHCO_3$, 0.36 mmol/L NaH_2PO_4 , 10 mmol/L glucose, 0.05 mmol/L Ca-Titriplex, and gassed with 95% O_2 , 5% CO_2 and pH 7.4 at 37 °C). After a further centrifugation step (900 g, 4 minutes), washed platelets were re-suspended in the same solution, allowed to equilibrate for 10 minutes at 37 °C and then stimulated with insulin (1 µmol/L) for 10 minutes. Some experiments were performed in platelets pre-treated with N^G-nitro-L-arginine methyl ester (L-NAME) (300 µmol/L, 30 minutes) for 30 minutes. After stimulation, the platelet suspension was centrifuged for 2 minutes at 900g and increasing doses of supernatant (0.1-0.2-0.4-0.8 ml) was added to phenyleprine-precontracted arteries mounted in an organ chamber (final volume, 15 ml). Total number and purity of platelets for each preparation was assessed by flow cytometry. Total protein from each preparation was also determined. Similar number of platelets ($174\pm19x10^6$/mL) between all samples was estimated.

To test the vasorelaxant effect evoked by platelet supernatants, studies of vascular reactivity on isolated vessels from C57BL/6 mice were carried out. Four ring segments (3 mm width) of thoracic aorta from each mouse were mounted between stainless steel triangles in a water-jacketed organ bath (37°C) for measurement of tension development as previously described [4]. Preliminary experiments demonstrated that the optimal resting tension for development of active contraction was 1g. Vessels were gradually stretched over one-hour period to this tension. The presence of functional endothelium and smooth muscle layer were assessed in all preparations by the ability respectively of acetylcholine

and nitroglycerine (10^{-9} to 10^{-5} mol/L) to induce the relaxation of vessels precontracted with phenylephrine (10^{-9} to 10^{-6} mol/L) to obtain a similar level of precontraction in each ring (80% of initial KCl-induced contraction). Responses to vasoconstrictors were examined at this resting tension and related to maximal vasoconstriction elicited by depolarization with 80 mmol/L KCl. Responses to vasodilator supernatants obtained from stimulation of platelets were examined after achieving a preconstricted tone with increasing doses of phenylephrine (10^{-9} to 10^{-6} mol/L) to obtain a similar level of precontraction in each ring (80% of initial KCl-induced contraction).

Measurement of platelet aggregation

Isolated platelets were centrifuged at 1500 g for 10 minutes and platelets were washed twice with a 6:1 mixture of Hank's balanced salt solution (HBSS) and Acid citrate dextrose (ACD).

Platelet-rich plasma (PRP) were incubated with 5, 15, 20, 25 or 50 mmol/L glucose or mannitol in the presence or absence of NSC23766 (15, 30, 50, 60, 75, 150 and 300 μM), EHT 1864 (Tocris Bioscience; 50 and 100 μM) or LY27632 for 30 minutes at 37°C. Platelet aggregation was monitored at 37°C with constant stirring (1200 rpm) in a dualchannel lumi-aggregometer (model 700; Chrono-Log). The maximum aggregation was expressed as a percentage of maximum light transmission, with unstimulated PPP being 0% and stimulated PRP 100%. Platelet aggregation was measured as the increase in light transmission for 5 minutes, with the addition of 0.8 μg/ml collagen, arachidonic acid (AA: 0.5 mM), adenosine diphosphate (ADP: 50 mM) or thrombin receptor-activating peptide (TRAP: 25μM) (Chrono-Log) as a proaggregatory stimuli.

Measurement of nitric oxide production in platelets

Platelet were resuspended (100 μL) in HBSS at room temperature and stimulated for 10 minutes with 1 μmol/L insulin. After incubation, the measurement of nitric oxide in platelets-supernatants were performed using NOAi Sievers 280 as described elsewhere.[5]

Rac1-GTP pull-down experiments.

Pooled mice mesenteric arteries, HUVECs, and human platelets were isolated as previous described. After glucose-exposure (5 or 25 mmol/L) or mannitol (5 or 25 mmol/L) or NSC23766 (30 μmol/L) or LY27632 (30 μmol/L) at 37°C, tissues or cells were lysed in a buffer containing NP-40 equipped by kit. In some platelets samples, after pre-incubation with glucose, mannitol, NSC23766 or LY27632, platelets were stimulated with 1 μg/ml collagen for 5 min. The reaction was terminated by the addition of an ice-cold EDTA (10 mmol/L) solution, followed by centrifugation at 10000g at 4°C for 2 minutes [6]. P21-binding domain (PBD) of p21-activated protein kinase (PAK) bound to agarose beads was added, and active Rac1, binding PAK1, was separated by repetitive centrifugation and washing. After, the specimens were boiled in Laemmli buffer, subjected to SDS-PAGE, and Rac was quantified by western blot analysis. In details, Rac1-GTP was detected with the monoclonal antibodies anti-Rac1-GTPγ (1:800; STA-401-1, Cells Biolab Inc.), and total Rac1 with monoclonal anti-Rac1 (1:1000; Abcam). Densitometry analysis was performed using Quantity One software (Bio-Rad Laboratories). The amount of Rac1-GTP was normalized to the total amount of Rac1 or GAPDH in mesenteric arteries or in cell lysates for the comparison of Rac1 activity (GTP-bound Rac1) among different samples.

Platelet fractionation

Blood was collected from the heart through cardiac puncture of isofluorane-anesthetized mice. PRP was prepared by addling 1-2 ml of saline to pooled blood and centrifuging the blood at 150 g for 10 min at ambient temperature. Platelets were quickly resuspended at 4° C in 1 mL of hypotonic buffer (5mM Tris-HCl/5mM EDTA, ph 7.5) and frozen in liquid nitrogen. Five cycles of rapid freezing and thawing lysed the cells, and the homogenate was centrifuged at 160000 g for 15 min. The resulting supernatant, representing the platelets cytosolic fraction, was rapidly removed and stored at -20° C. At this point, the pellets were resuspended in 300 μL of Tris/EDTA buffer, and 50 μL of this mixture was layered on top of 100 μL of a solution contained 27% (wt/vol) sucrose, 10mM

This-HCl, 1 mM EDTA and phenylmethylsulfonyl fluoride (45 µg/mL) in each microcentrifuge tubes. After centrifugation at 160000 g for 2 min, the membrane fractions were observed as two faint bands at the top of the sucrose layer. Membrane fractions were carefully aspirated and diluted in buffer Tris/EDTA. Finally, cytosolic and membrane fractions were use to immunoblotting analyses.

Immunoblotting

Platelets, pooled vessels or cells were solubilized in lysis buffer containing: 20 mmol/L Tris-HCl, 150 mmol/L NaCl, 20 mmol/L NaF, 2 mmol/L sodium orthovanadate, 1% Nonidet, 100 µg/ml leupeptin, 100 µg/ml aprotinin, and 1 mmol/L phenylmethylsulfonyl fluoride. Then, samples were left on ice for 30 minutes and centrifuged at 10621 g for 20 minutes, and the supernatants were used to perform immunoblot analysis. Total protein levels were determined using the Bradford method. Rac1 activity was determined using a commercially available kit (Cell BioLabs Inc. STA-401-1). 50 micrograms of proteins were resolved on 12% SDS-PAGE, transferred to a nitrocellulose membrane and immunoblotted with anti-Rac1-GTP (1:1000, Cell BioLabs) or with anti-Rac1 (1:1000, Abcam); anti-ROCK1 (1:800, Abcam); anti-p-eNOS or anti-eNOS (1:800, Abcam); anti-p-PI3K (1:800, Thermo Fisher); anti-PI3K (1:1000, Thermo Fisher); anti-PAK1 (1:800, Thermo Fisher); anti-p-Akt (1:800, Santa Cruz); anti-Akt (1:1000, Santa Cruz); anti-RhoA-GTP (NewEast Biosciences); anti-RhoA (Thermo Fisher) and anti-β-Actin (1:1000, Cell signaling) anti CD62 (1:800, Abcam), anti Na/K-ATPase (1:1000, Cell signaling). HRP-conjugated secondary antibodies were used at 1:3000 dilution (Bio-Rad Laboratories). Protein bands were detected by ECL Prime (Amersham Biosciences) and densitometry analysis was performed using Quantity One software (Bio-Rad Laboratories).

RNA extraction and quantitative real-time PCR

Total RNA from tissue samples was extracted using TRIzol reagent (Invitrogen). Quantitative real-time PCR (qRT-PCR) assays were carried out to detect mRNA expression using the PrimeScript RT Reagent Kit (TaKaRa) and SYBR Premix Ex Taq (TaKaRa) according to the manufacturer's

instructions. The levels of *ROCK1* transcript were measured by forward primer: TCTCATTTGTGCCTTCCTTAC, and reverse primer: ACTGGTGCTACAGTGTCT. β-Actin was used as an internal control.

SUPPLEMENTAL FIGURES

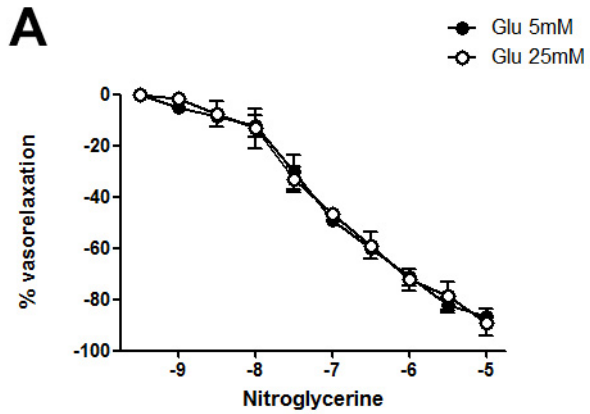

Supplemental Figure 1. A) Nitroglycerine-evoked vasorelaxation in pre-constricted mesenteric arteries (n=4 for each group) treated with low (Glu 5mM, full circles) and high glucose levels (Glu 25 mM, empty circles).

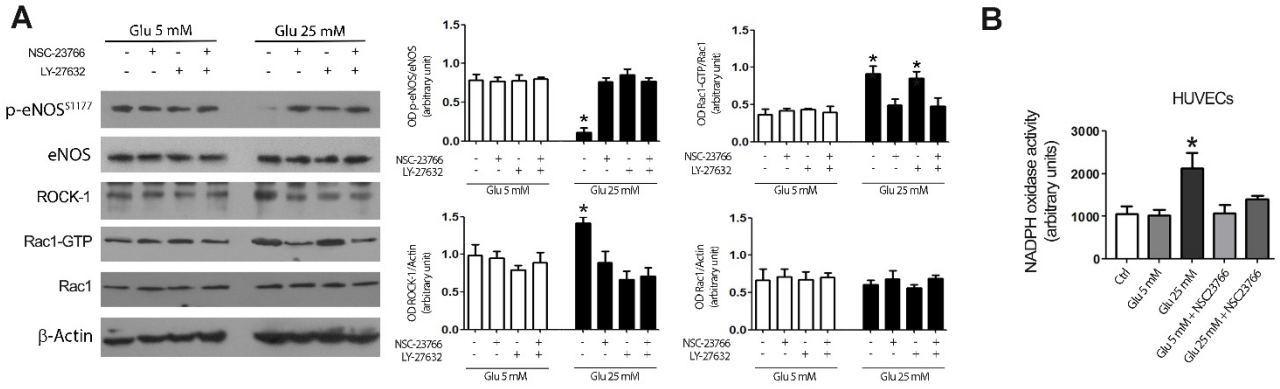

Supplemental Figure 2. A) Representative immunoblot (left) and densitometric analysis (right) of p-eNOS, eNOS, ROCK1, Rac1-GTP, Rac1 and β-actin in serum-starved HUVECs treated with 5mM or 25mM of glucose, stimulated with acethylcholine. Cells have been treated with NSC23766 alone, with LY27632 alone or concomitantly with both compound. The data are presented as mean ±SEM from three independent experiments.* $p<0.05$ vs. all. **B)** Effects of glucose and Rac1 inhibitor treatment on NADPH oxidase activity in HUVECs. Levels of NADPH activity was measured by lucigenin-enhanced chemiluminescence. 4 independent experiments. * $p<0.05$ vs all.

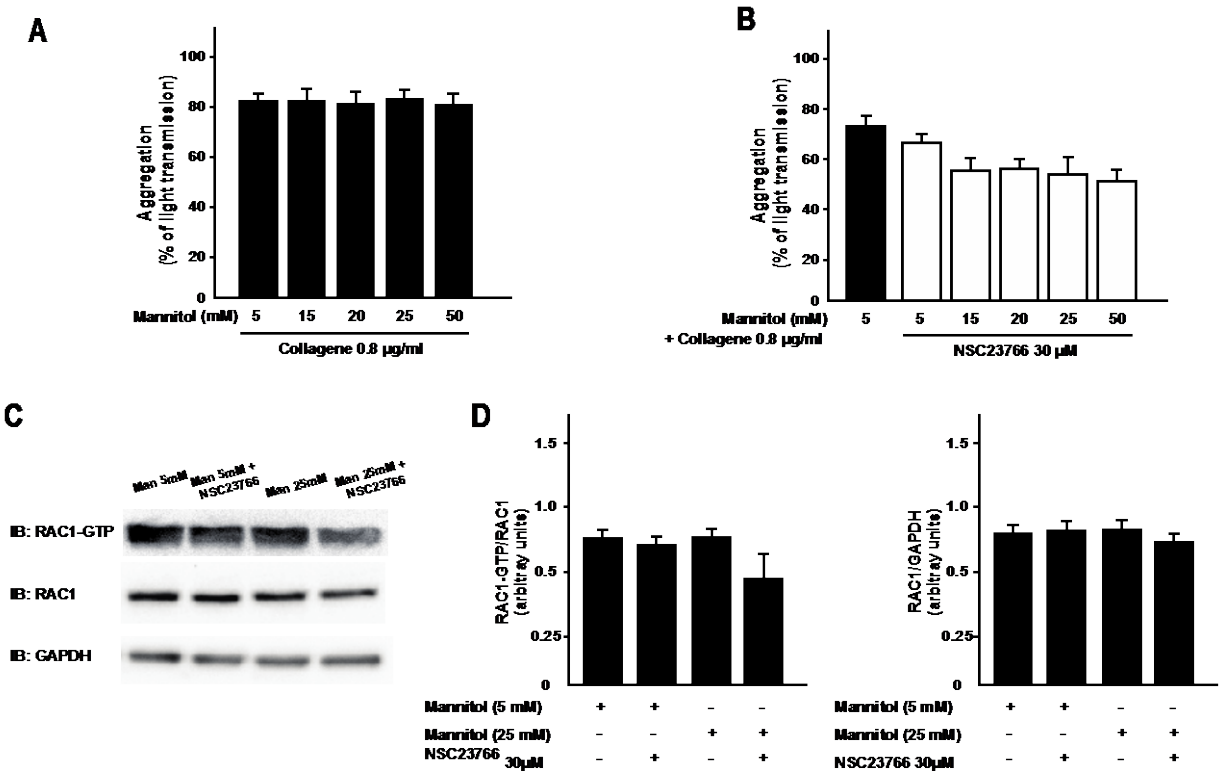

Supplemental Figure 3. A) Quantification of platelets aggregation presented as percentage of light transmission of platelets from control subjects treated with increasing concentrations of mannitol. Data are expressed as mean ± SEM. n= 4 independent experiments from individual subjects **B)** Quantification of platelets aggregation presented as percentage of light transmission of platelets from control subjects treated with manitol plus increasing concentrations of NSC23766. Data are presented as mean ± SEM. n= 4 independent experiments from individual subjects **C)** Representative immunoblot of Rac1 and Rac1-GTP levels in platelets from control subjects (CTRL) treated with mannitol 5mM and 25 mM plus NSC23766, **(D)** and relative densitometric analysis. n= 4 independent experiments from individual subjects

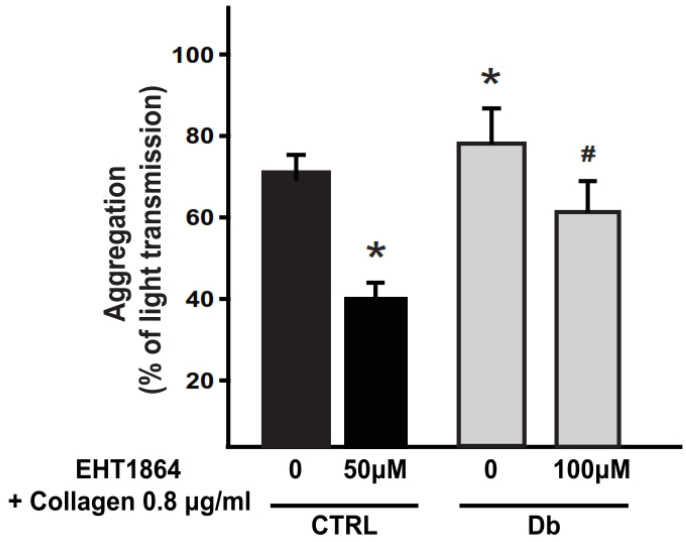

Supplemental Figure 4. Quantification of platelets aggregation presented as percentage of light transmission of platelets from control (CTRL) and diabetic (Db) subjects treated with two different dose of EHT1864. n= 4 independent experiments from individual subjects. *p<0.05 vs. CTRL 0 (without EHT1864), #p<0.05 vs. Db 0 (without NSC23766).

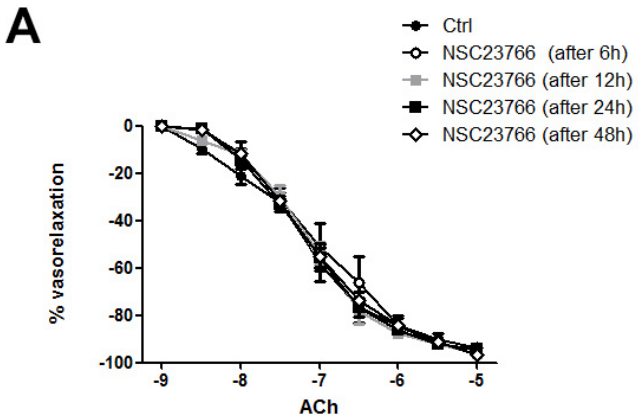

Supplemental Figure 5. A) Acetylcholine (ACh) vasorelaxation in preconstricted mice mesenteric arteries in basal condition (Ctrl, full circle) and after i.p. treatment with Rac1 inhibitor, NSC23766 5mg/Kg, at different timepoints (6-12-24-48 hours) (n=4 for each group).

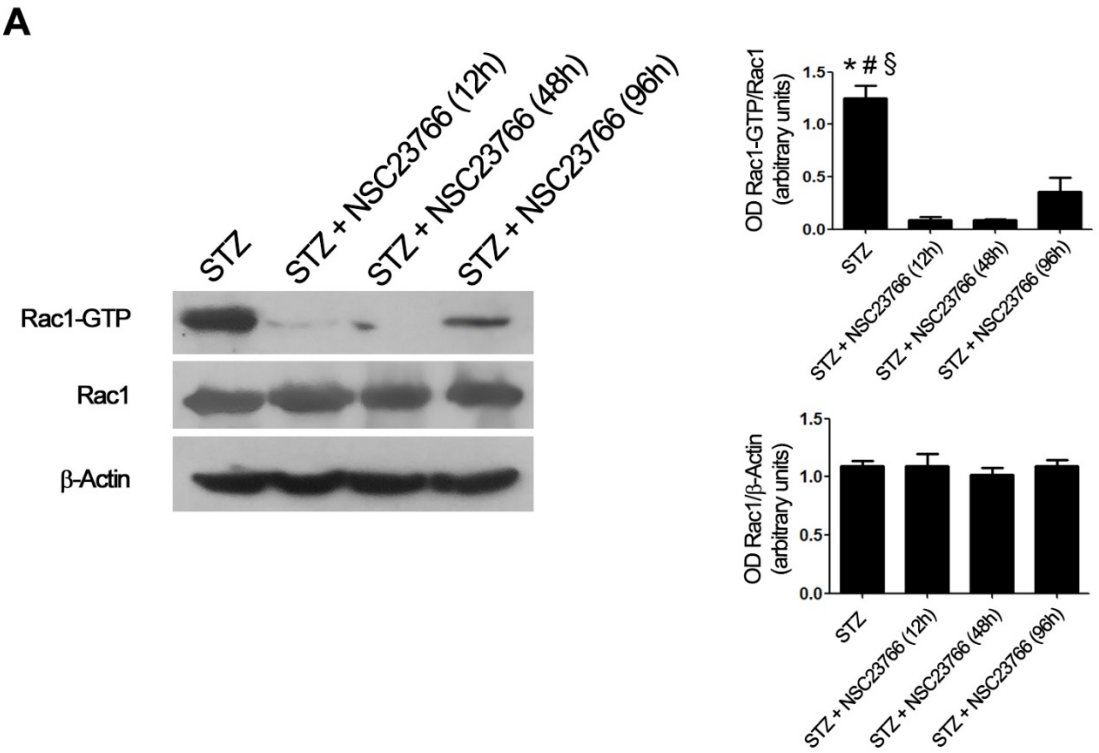

Supplemental Figure 6. A) Representative immunoblot (*left*) anddensitometric analysis (*right*) of Rac1-GTP, total Rac1 and β-Actin levels in mesenteric arteries from streptozotocin-treated mice injected i.p. with NSC23766 (5mg/Kg) and evaluated at different timepoints (12,48,96 hours). n= 3 independent experiments. * $p<0.05$ vs STZ + NSC23766 (12h); $^{\#}$ $p<0.05$ vs STZ + NSC23766 (48h); § $p<0.05$ vs STZ + NSC23766 (96h).

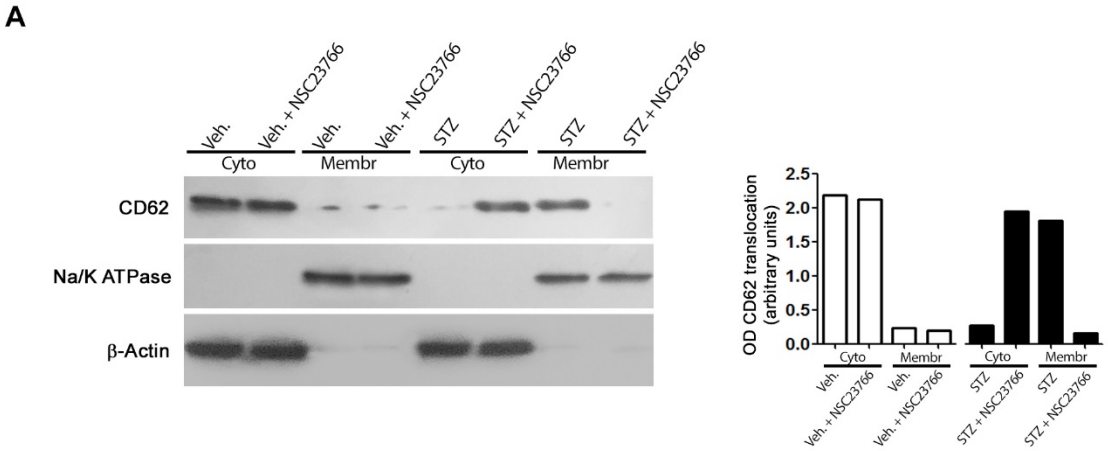

Supplemental Figure 7. A) Representative immunoblots (*left*) and densitometric analysis (*right*) showing protein levels of CD62, Na/K ATPase, and β-Actin in subcellular fractions (cytosol and membranes) of platelets isolated from STZ- and vehicle- treated mice in presence or absence of NSC23766. Na/K ATPase and β-Actin were used as membrane and cytoplasmic markers, respectively.

SUPPLEMENTAL TABLES

Supplemental Table 1.

	DIABETICS WITHOUT ASA (n=15)	**DIABETICS WITH ASA (n=7)**
HbA1c ≥ 10%	4	0
7%≤HbA1c <10%	7	5
HbA1c <7%.	4	2

Abbreviations used: ASA= acetylsalicylic acid; HbA1c = glycohemoglobin.

Supplemental Table 2.

Animal groups [n]	***Blood glucose [mg/dL]***	***Body weight [grams]***
Control [8]	*125 ± 11*	*27.6 ± 0.9*
STZ [10]	*453 ± 18**	*24.1 ± 0.5*
STZ + NSC23766 [8]	*464 ± 13**	*24.3 ± 0.4*
Vehicle [8]	*128 ± 9*	*28.1 ± 0.7*
Vehicle + NSC23766 [8]	*122 ± 14*	*27.8 ± 0.5*

Characteristics of diabetic mice used in the study. Abbreviations: [n]=numbers; Mice received STZ dissolved in 0.1 M citrate buffer (STZ) or a solution of 0.1 M citrate buffer alone (vehicle). Control, untreated mice; STZ, streptozotocin-treated mice; STZ + NSC23766, streptozotocin-treated mice plus NSC23766; Vehicle, mice treated with sodium citrate buffer alone; Vehicle + NSC23766, mice treated with sodium citrate buffer alone plus NSC23766. *$p<0.05$ vs. vehicle and vehicle plus NSC23766.

Supplemental References

1. Zhang S, Rahman M, Song L, Herwald H and Thorlacius H. Targeting Rac1 signaling inhibits streptococcal M1 protein-induced CXC chemokine formation, neutrophil infiltration and lung injury. *PloS one*. 2013;8:e71080.

2. Hwaiz R, Hasan Z, Rahman M, Zhang S, Palani K, Syk I, Jeppsson B and Thorlacius H. Rac1 signaling regulates sepsis-induced pathologic inflammation in the lung via attenuation of Mac-1 expression and CXC chemokine formation. *The Journal of surgical research*. 2013;183:798-807.

3. Classification and diagnosis of diabetes mellitus and other categories of glucose intolerance. National Diabetes Data Group. *Diabetes*. 1979;28:1039-57.

4. Carrizzo A, Di Pardo A, Maglione V, Damato A, Amico E, Formisano L, Vecchione C and Squitieri F. Nitric oxide dysregulation in platelets from patients with advanced Huntington disease. *PloS one*. 2014;9:e89745.

5. Carrizzo A, Lenzi P, Procaccini C, Damato A, Biagioni F, Ambrosio M, Amodio G, Remondelli P, Del Giudice C, Izzo R, Malovini A, Formisano L, Gigantino V, Madonna M, Puca AA, Trimarco B, Matarese G, Fornai F and Vecchione C. Pentraxin 3 Induces Vascular Endothelial Dysfunction Through a P-selectin/Matrix Metalloproteinase-1 Pathway. *Circulation*. 2015;131:1495-505; discussion 1505.

6. Kageyama Y, Doi T, Akamatsu S, Kuroyanagi G, Kondo A, Mizutani J, Otsuka T, Tokuda H, Kozawa O and Ogura S. Rac regulates collagen-induced HSP27 phosphorylation via p44/p42 MAP kinase in human platelets. *International journal of molecular medicine*. 2013;32:813-8.